Simulation of "Extreme Fluids"

Examples, Challenges and Simulation Techniques for Flow Problems with Complex Rheology

H. Damanik, J. Hron, A. Ouazzi, M. Razzaq, S. Turek
Institut für Angewandte Mathematik, LS III, TU Dortmund
http://www.mathematik.tu-dortmund.de/lsiii

What are „Extreme“ Fluids?

Complex rheology with „extreme“ changes of viscosity:

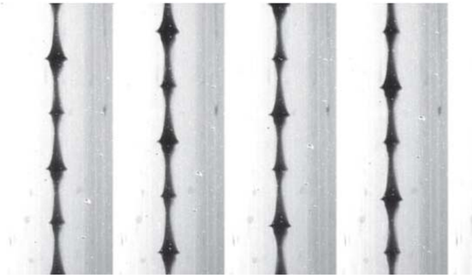

- **Dependence of shear rate, pressure and temperature**

→ Generalized Newtonian, resp., non-Newtonian rheology

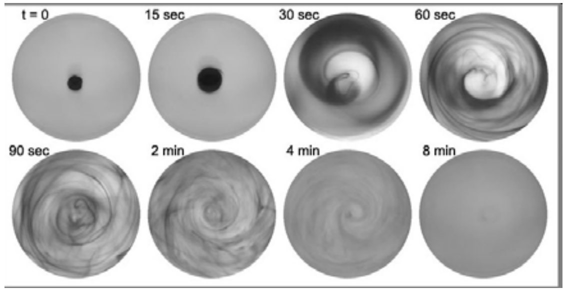

- **Viscoelastic effects**

→ Extra-Polymer stress („turbulence“)

- **Many interacting objects in the fluid**

→ Suspensions as particulate flow

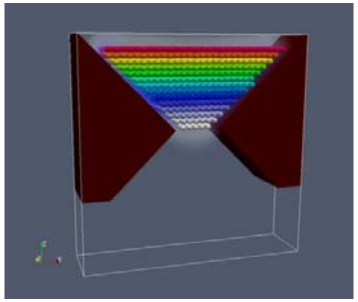

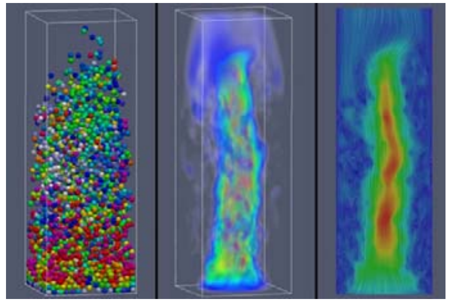

- **Special discretization/stabilization required**
- **Special solution techniques required**
- **Special software techniques required**

Black Box???

Realization in *FeatFlow*

HPC features:
- Moderately parallel
- GPU computing
- Open source


Hardware -oriented Numerics

Numerical features:
- Higher order (Q2P1) FEM in space & (semi-) Implicit FD/FEM in time
- Semi-(un)structured meshes with dynamic adaptive grid deformation
- Fictitious Boundary (FBM) methods
- Newton-Multigrid-type solvers

Non-Newtonian flow module:
- generalized Newtonian model (Power-law, Carreau,...)
- viscoelastic model (Giesekus, FENE, Oldroyd,...)

Multiphase flow module (resolved interfaces):
- ℓ/ℓ – interface capturing (Level Set)
- s/ℓ – interface tracking (FBM)
- $s/\ell/\ell$ – combination of ℓ/ℓ and s/ℓ

Engineering aspects:
- Geometrical design
- Modulation strategy
- Optimization

Here: FEM-based tools for the accurate simulation of (multiphase) flow problems, particularly with complex rheology

Example: Screw Extruder (I)

- Numerical simulation of *(twin)screw extruders* for *polymer processing*
- *Non-Newtonian rheological* models (shear & temperature dependent) with *non-isothermal* conditions (cooling from outside, heat production)
- Analysis of the influence of local characteristics on the global product quality, prediction of hotspots and maximum shear rates
- Optimization of torque acting on the screws, energy consumption

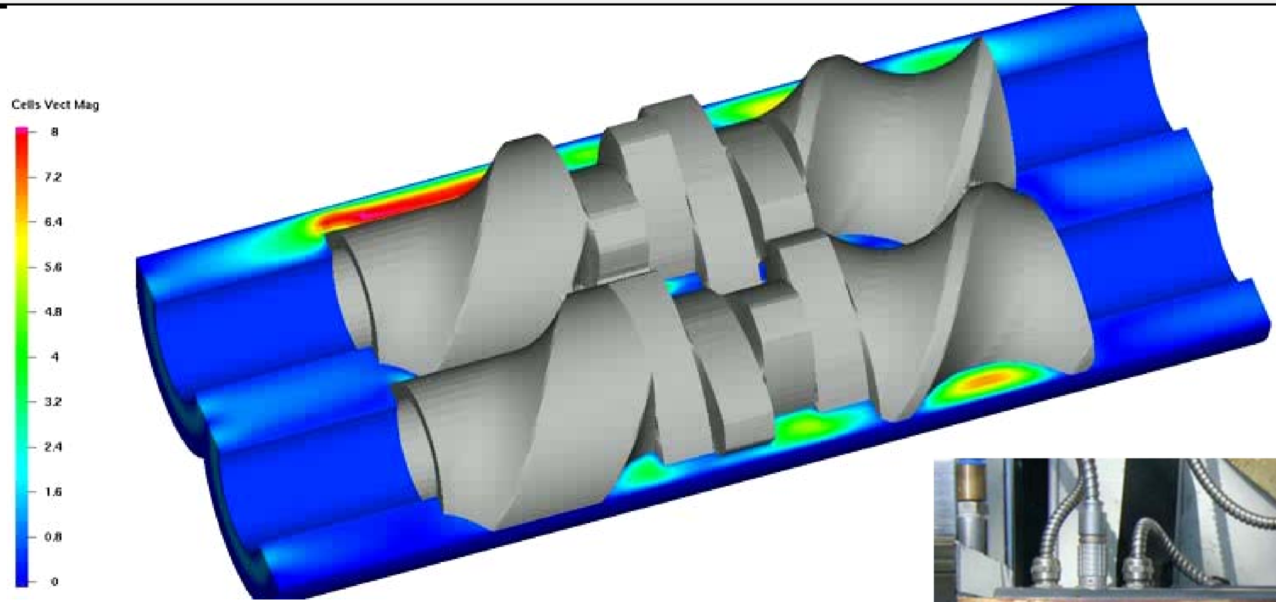

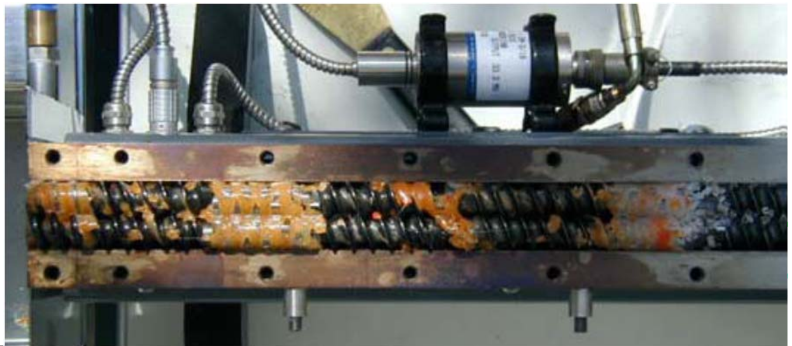

Example: Screw Extruder (II)

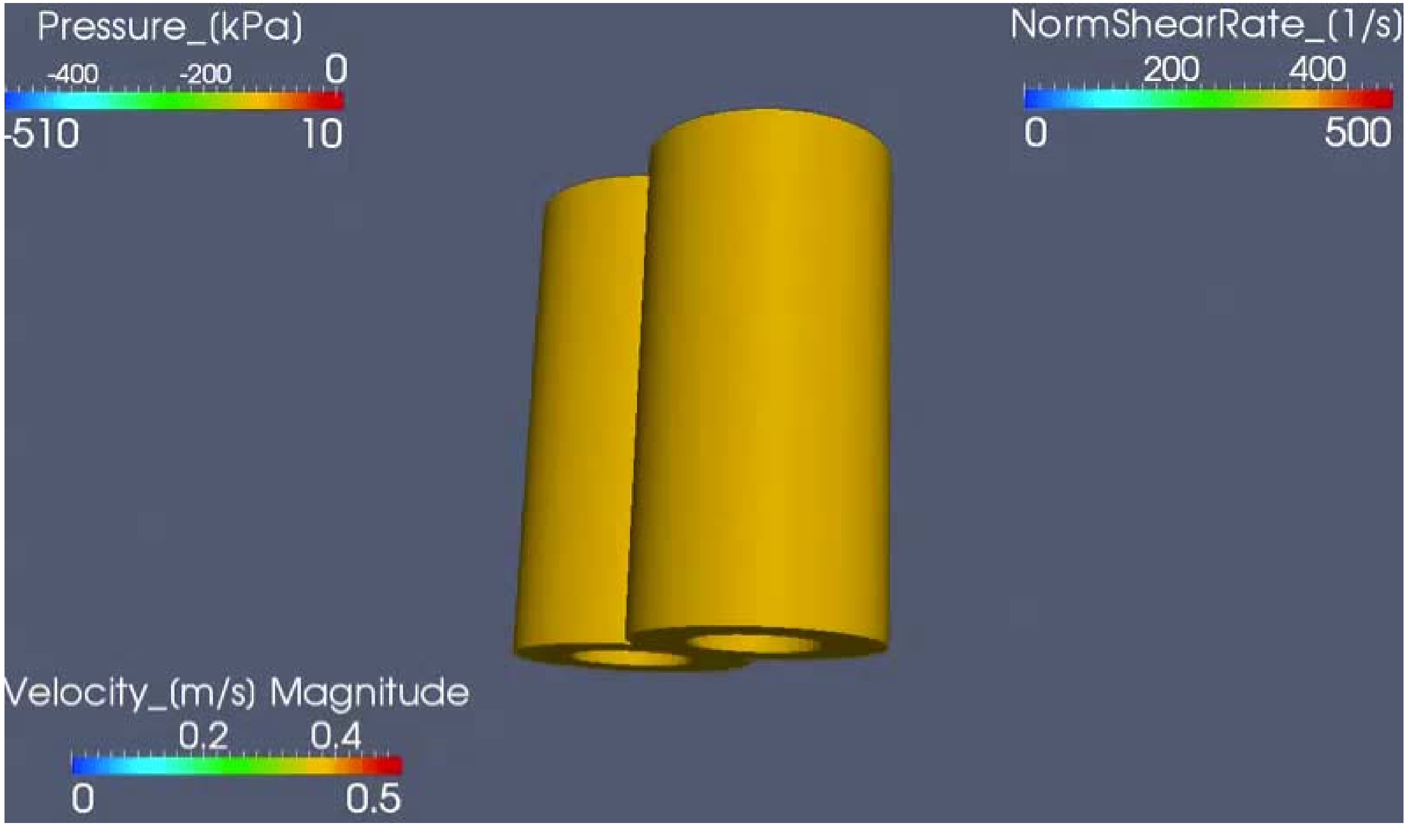

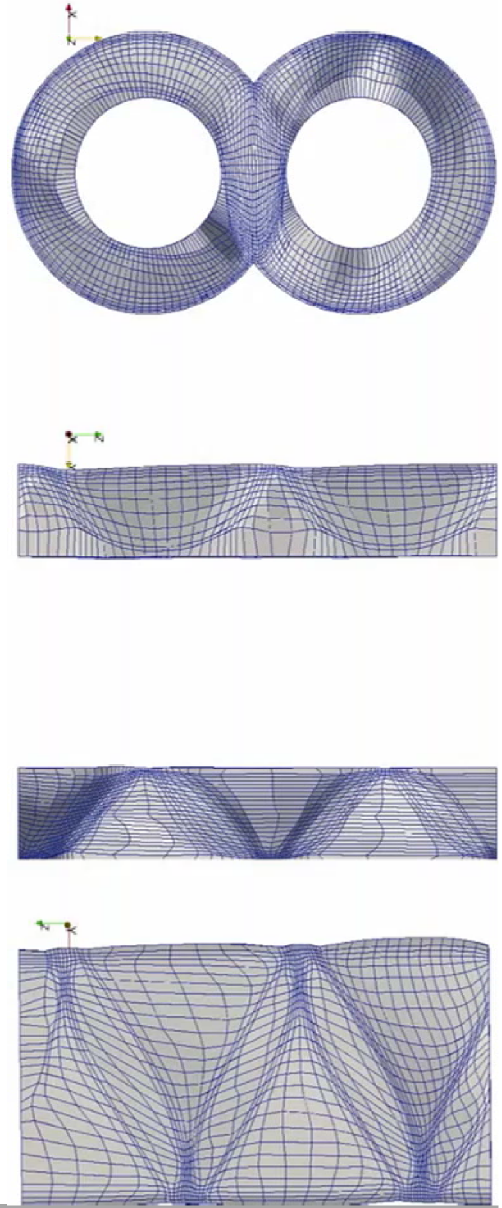

Example: Screw Extruder (III)

technische universität dortmund

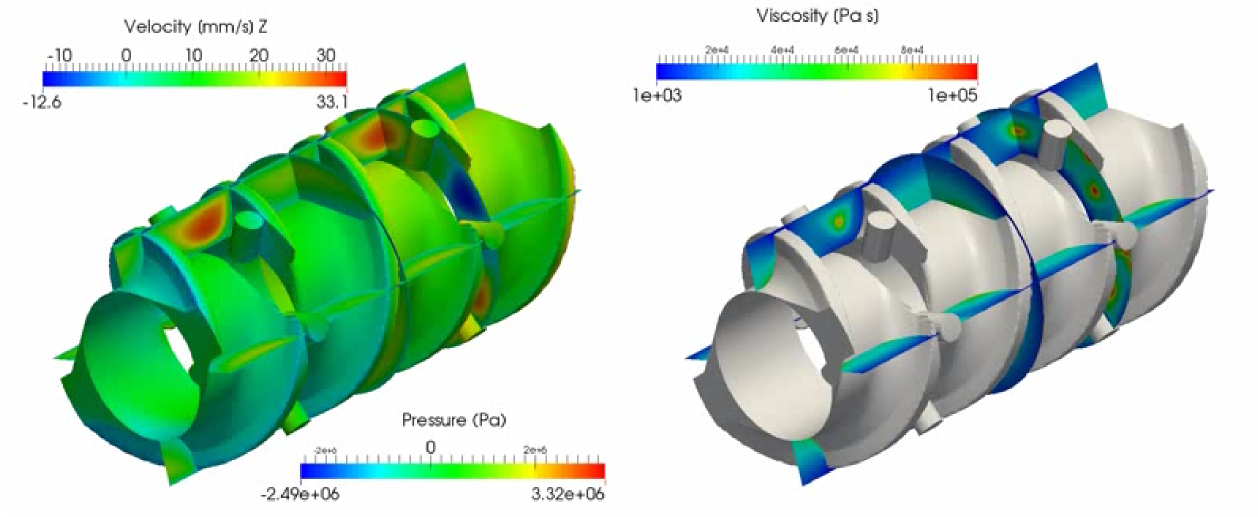

Twin-screw-element library

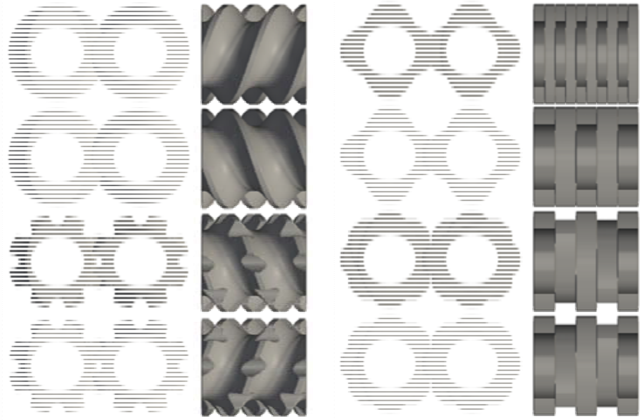

Combination of screw segments

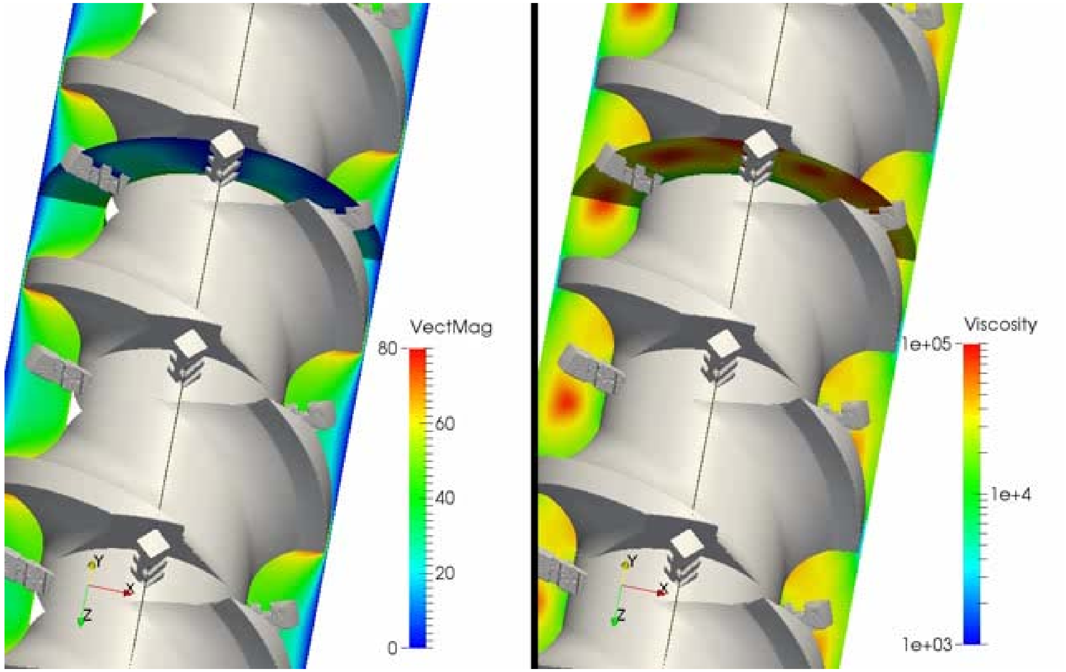

Governing Equations

technische universität dortmund

- **Generalized Navier-Stokes equations**

$$\rho\left(\frac{\partial}{\partial t} + u \cdot \nabla\right)u = -\nabla p + \nabla \cdot \sigma, \quad \nabla \cdot u = 0,$$

$$\rho c_p\left(\frac{\partial}{\partial t} + u \cdot \nabla\right)\Theta = k_1 \nabla^2 \Theta + k_2 \mathrm{D} : \mathrm{D},$$

$$D(u) = \frac{1}{2}\left(\nabla u + (\nabla u)^T\right),$$

$$\sigma = \sigma_s + \sigma_p .$$

- **Viscous stress**

$$\sigma_s = 2\eta_s(\dot{\gamma}, \Theta, p)D, \quad \dot{\gamma} = \sqrt{\mathrm{tr}(D(u)^2)}.$$

- **Elastic stress**

$$f_1(L, \sigma_p)\sigma_p + \Lambda \overset{\nabla}{\sigma}_p + F_2(\sigma_p, D) + F_3(\sigma_p) = 2\eta_p D(u).$$

- **Viscous stress**

$$\sigma_s = 2\eta_s(\dot{\gamma}, \Theta, p)D, \ \dot{\gamma} = \sqrt{\mathrm{tr}(D(u)^2)}.$$

- **Power Law model**

$$\eta_s(\dot{\gamma}, \Theta, p) = \eta_0(\varepsilon + \dot{\gamma}^2)^{(\frac{r}{2}-1)}, \ (\eta_0 > 0, r > 1).$$

- **Generalized Cross model**

$$\eta_s(\dot{\gamma}, \Theta, p) = \eta_\infty + \frac{(\eta_0 - \eta_\infty)}{(1+(\lambda\dot{\gamma})^{r_1})^r}\exp(\alpha p + (a_1 + \frac{a_2}{a_3 + \Theta})),$$

$$(\eta_0 > \eta_\infty \geq 0, \ r > 1, \lambda > 0).$$

Constitutive Models (II)

- **Generalized upper convective constitutive model**

$$f_1(L_k, tr(\sigma_p), \Lambda, \eta_p)\sigma_p + \Lambda \overset{\nabla}{\sigma}_p + F_2(\sigma_p, D) + F_3(\sigma_p) = 2\eta_p D(u),$$

$$\overset{\nabla}{\sigma}_p := \frac{\partial \sigma_p}{\partial t} + u \cdot \nabla \sigma_p - \nabla u \cdot \sigma_p - \sigma_p \cdot \nabla u^T.$$

	f_1	F_2	F_3
Oldroyd-B/UCM	1	0	0
Giesekus	1	0	$\alpha\sigma_p^2$
FENE-P/-CR	$f_1(L_k, tr(\sigma_p))$	0	0
White & Metzner $\Lambda = \Lambda(\dot{\gamma}), \eta_p = \eta_p(\dot{\gamma})$	1	0	0
PTT	$f_1(\eta_p, tr(\sigma_p), \Lambda)$	$\xi(D\sigma_p + \sigma_p D)$	0
Pom-Pom	$f_1(tr(\sigma_p), \Lambda)$	$F_2(G, \sigma_p, \Lambda)$	$F_3(G, \sigma_p^2, \alpha)$

Constitutive Models (III)

- **Exemplary model: White-Metzner**

$$\sigma_p + \Lambda(\dot{\gamma})\overset{\nabla}{\sigma}_p = 2\eta_p(\dot{\gamma},\Theta,p)D(u), \qquad \dot{\gamma} = \sqrt{2D(u):D(u)}$$

- **Larson:**

$$\Lambda(\dot{\gamma}) = \frac{\Lambda}{1+a\Lambda\dot{\gamma}} \qquad \eta_p(\dot{\gamma},\Theta,p) = \frac{\eta_p}{1+a\Lambda\dot{\gamma}}$$

- **Cross:**

$$\Lambda(\dot{\gamma}) = \frac{\Lambda}{1+(L\dot{\gamma})^{1-n}} \qquad \eta_p(\dot{\gamma},\Theta,p) = \frac{\eta_p}{1+(k\dot{\gamma})^{1-m}}$$

- **Carreau-Yasuda:**

$$\Lambda(\dot{\gamma}) = \Lambda\left[1+(L\dot{\gamma})^b\right]^{\frac{n-1}{b}} \qquad \eta_p(\dot{\gamma},\Theta,p) = \eta_p\left[1+(k\dot{\gamma})^a\right]^{\frac{m-1}{a}}$$

Numerical Challenges

- **Discretizations have to handle the following challenges points**
  - **Stable FEM spaces for velocity/pressure and velocity/stress interpolation** $Q_2/Q_2/P_1^{disc}$ **or** $\tilde{Q}_1/\tilde{Q}_1/P_0$ **or** $\tilde{Q}_2/\tilde{Q}_2/P_1^{disc}$
  - **Special treatment of the convective terms: edge-oriented/interior penalty (EO-FEM), TVD/FCT**
  - **High Weissenberg number problem (HWNP): LCR (Reformulation)**
  - **Locally adapted meshes due to steep gradients: GDM**

- **Solvers have to deal with different sources of nonlinearity**
  - **Nonlinearity: Newton method**
  - **Strong coupling of equations: monolithic multigrid approach**

- **Complex geometries (and meshes)**
  - **FBM + distance based Level Set FEM for free interfaces**

Problem Reformulation (I)

technische universität dortmund

Elastic stress → (u, p, σ_p)

$$\left.\begin{aligned} &\rho\left(\frac{\partial}{\partial t} + u\cdot\nabla\right)u = -\nabla p + 2\nabla\cdot\eta_s D + \nabla\cdot\sigma_p, \quad \nabla\cdot u = 0 \\ &f_1(L,\sigma_p)\sigma_p + \Lambda\overset{\nabla}{\sigma}_p + F_2(\sigma_p, D) + F_3(\sigma_p) = 2\eta_p D(u) \end{aligned}\right\} \quad \textbf{(1)}$$

Conformation stress → (u, p, σ_c) is positive definite by design !!

Replace σ_p in (1) with $\sigma_p = \dfrac{\eta_p}{\Lambda}(\sigma_c - I)$ → special discretization: TVD

$$\left.\begin{aligned} &\rho\left(\frac{\partial}{\partial t} + \mathrm{u}\cdot\nabla\right)u = -\nabla p + 2\nabla\cdot\eta_s D + \frac{1}{\Lambda}\nabla\cdot\eta_p\sigma_c, \quad \nabla\cdot\mathrm{u} = 0, \\ &\overset{\nabla}{\sigma}_c + F_4(\sigma_c, u) = 0 \end{aligned}\right\} \quad \textbf{(2)}$$

Problem Reformulation (II)

$$\sigma_c(t) = \int_{\infty}^{t} \frac{1}{\mathrm{We}^2} \exp\left(\frac{-(t-s)}{\mathrm{We}} \right) F(s,t) F(s,t)^T \, ds$$

Positive by design,
so we can take its logarithm

2 Observations:

- positive definite → special discretizations like FCT/TVD
- exponential behaviour → approximation by polynomials???

Driven Cavity:
as We number changes from We=0.5 to We=1.5, the stress value jumps significantly

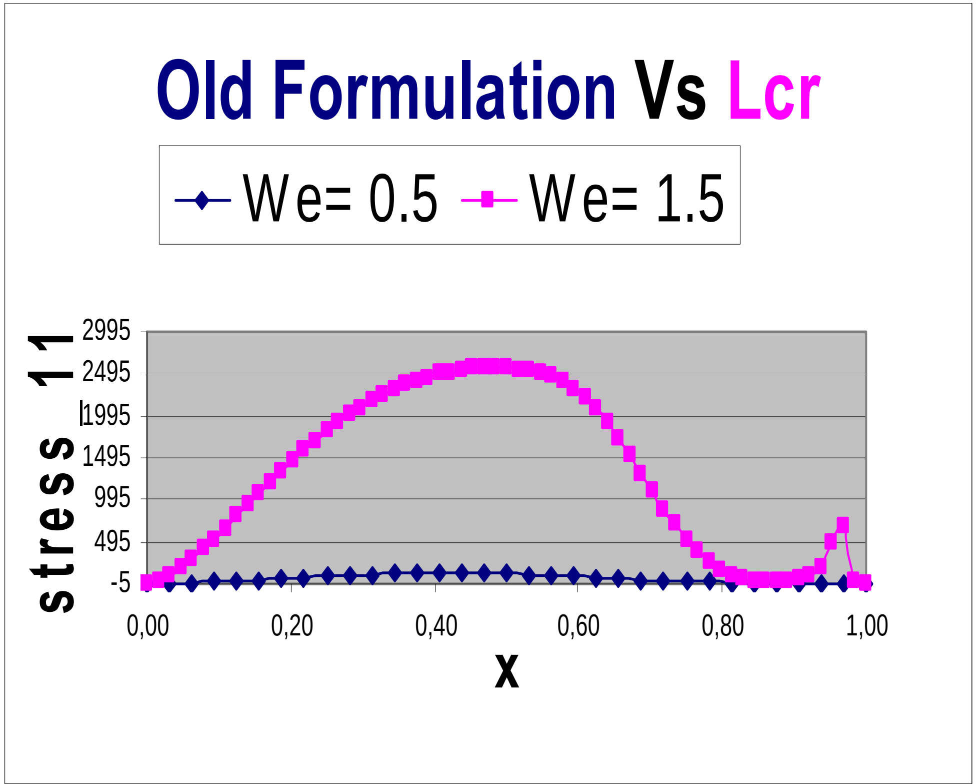

Cutline of Stress_11 component at y = 1.0

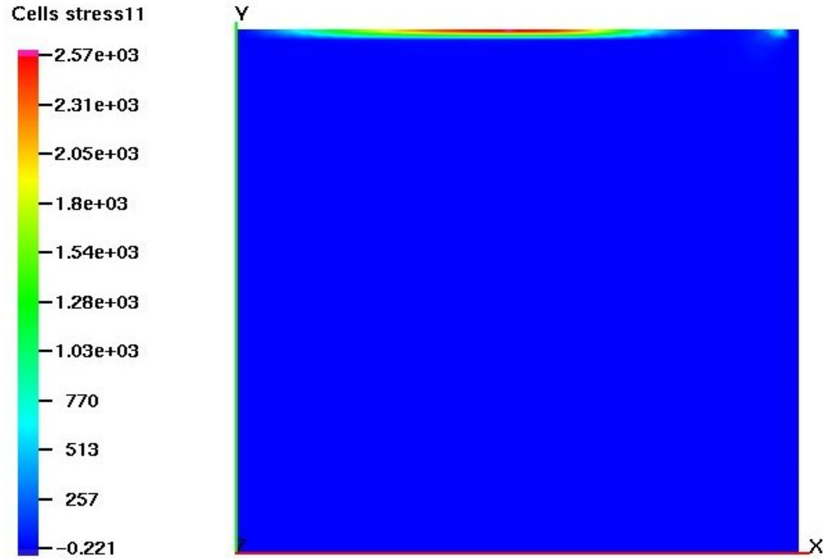

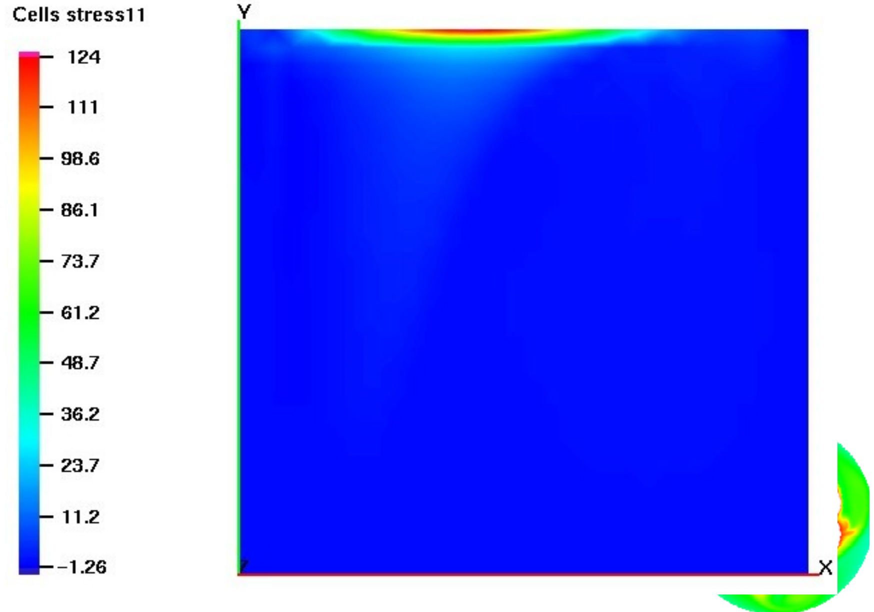

Problem Reformulation (IV)

technische universität dortmund

- **Experience:**
  - Stresses grow exponentially
  - Conformation tensor is positive by design

- **Fattal and Kupferman:**
  - **Take the logarithm** as a new variable $\sigma_{LCR} = \log \sigma_c$ using the eigenvalue decomposition

$$\sigma_{LCR} = R \log(\lambda_{\sigma_c}) R^T$$

  - Decompose the velocity gradient inside the stretching part

$$\nabla u = B + \Omega + N \sigma_c^{-1}$$

Remark for PTT only $L = B + \Omega + N \sigma_c^{-1}, \; L = \nabla u - \xi D$

LCR can be applied to all upper convective models

Problem Reformulation (V)

$$f_1(L,\sigma_p)\sigma_p + \Lambda \overset{\nabla}{\sigma}_p + F_2(\sigma_p, D) + F_3(\sigma_p) = 2\eta_p D(u)$$

$$\sigma_p = \frac{\eta_p}{\Lambda}(\sigma_c - I)$$

$$\overset{\nabla}{\sigma}_c + F_4(\sigma_c, u) = 0$$

$$\nabla u = \Omega + B + N\sigma_c^{-1}$$

$$\left(\frac{\partial}{\partial t} + u \cdot \nabla\right)\sigma_c - (\Omega\sigma_c - \sigma_c\Omega) + 2B\sigma_c = \frac{1}{\Lambda}(\mathrm{I} - \sigma_c)$$

$$\sigma_c = \exp \sigma_{LCR}$$

$$\sigma_{LCR} = R \log(\lambda_{\sigma_c})\, R^T$$

$$\left(\frac{\partial}{\partial t} + u \cdot \nabla\right)\sigma_{LCR} - (\Omega\sigma_{LCR} - \sigma_{LCR}\Omega) - 2B = F_4(\sigma_{LCR}, u).$$

Full Set of Equations

- **Generalized Newtonian (VP)**

$$\rho\left(\frac{\partial}{\partial t}+u\cdot\nabla\right)u=-\nabla p+\nabla\cdot\left(2\eta_s(\dot{\gamma},\Theta,\,p)D(u)\right)+\frac{1}{\Lambda}\nabla\cdot\eta_p e^{\sigma_{LCR}},\quad \nabla\cdot u=0,$$

- **Non-isothermal effect (T)**

$$\rho c_p\left(\frac{\partial}{\partial t}+u\cdot\nabla\right)\Theta=k_1\,\nabla^2\Theta+k_2\mathrm{D}:\mathrm{D},$$

- **LCR equation (S)**

$$\left(\frac{\partial}{\partial t}+u\cdot\nabla\right)\sigma_{LCR}-\left(\Omega\sigma_{LCR}-\sigma_{LCR}\Omega\right)-2B=F_4\left(\sigma_{LCR},u\right).$$

$F_4\left(\sigma_{LCR},u\right)$ **Refers to all upper convective constitutive models**

Examplary Viscoelastic Models

technische universität dortmund

Oldroyd-B/UCM $$F_4 = \frac{1}{\Lambda}(e^{-\sigma_{LCR}} - I)$$

Giesekus $$F_4 = \frac{1}{\Lambda}(e^{-\sigma_{LCR}} - I - \alpha e^{\sigma_{LCR}} - (e^{-\sigma_{LCR}} - I)^2)$$

FENE-P/-CR $$F_4 = \frac{1}{\Lambda} f(R)(e^{-\sigma_{LCR}} - I) \Big/ F_4 = \frac{1}{\Lambda}(e^{-\sigma_{LCR}} - f(R)I)$$

White-Metzner $$F_4 = \frac{1}{\Lambda(\dot{\gamma})}(e^{-\sigma_{LCR}} - I)$$

Linear PTT $$F_4 = \frac{1}{\Lambda}(1 + \varepsilon(tr(e^{\sigma_{LCR}} - 3)))(e^{-\sigma_{LCR}} - I)$$

Exponential PTT $$F_4 = \frac{1}{\Lambda}\exp(\varepsilon(tr(e^{\sigma_{LCR}} - 3)))(e^{-\sigma_{LCR}} - I)$$

Pom-Pom $$F_4 = -\frac{1}{\Lambda}([f(\sigma_{LCR}) - 2\alpha]e^{\sigma_{LCR}} + \alpha e^{2\sigma_{LCR}} + (\alpha - 1)I)$$

FEM Discretization

- **High order $Q_2 / Q_2 / P_1^{disc}$ for velocity-stress-pressure**

  - **Advantages:**
    - **Inf-sup stable for velocity and pressure**
    - **High order: good for accuracy**
    - **Discontinuous pressure: good for solver & physics**

  - **Disadvantages:**
    - **Stabilization for same spaces for stress-velocity**
    - **a single d.o.f. belongs to four elements (in 2D)**

Compatibility condition between the stress and velocity spaces via EO-FEM

Variational Formulations

technische universität dortmund

- **Standard Navier-Stokes bilinear forms**

$$a(u,v) = \int_\Omega \frac{1}{\Delta t} u \cdot v \, d\Omega + \int_\Omega 2\eta_s D(u) : D(v) \, d\Omega$$

$$b(p,v) = -\int_\Omega p \, \nabla \cdot v \, d\Omega$$

- **Nonsymmetric bilinear forms due to LCR**

$$c(\sigma_{LCR}, v) = \int_\Omega \exp(\sigma_{LCR}) : D(v) \, d\Omega$$

$$\tilde{c}(\tau, u) = -2\int_\Omega B(\nabla u, \sigma_c) : \tau \, d\Omega$$

- **Nonlinear tensor variational form due to LCR**

$$d(\sigma_{LCR}, \tau) = \int_\Omega \left(\frac{1}{\Delta t} + (u \cdot \nabla) \right) \sigma_{LCR} : \tau \, dx$$

$$- \int_\Omega (\Omega \sigma_{LCR} - \sigma_{LCR} \Omega) : \tau \, dx - \int_\Omega F_4 (\sigma_{LCR}, u) : \tau \, dx$$

- **Nonsymmetric bilinear forms due to LCR**

$$e(\Theta, \Phi) = \int_\Omega \left(\frac{1}{\Delta t} + u \cdot \nabla \right) \Theta \Phi \, dx + \int_\Omega k \nabla \Theta \cdot \nabla \Phi \, dx$$

$$- \int_\Omega 2\eta_s [D(u) : D(u)] \Phi \, dx - \int_\Omega D(u) : \exp(\sigma_{LCR}) \Phi \, dx$$

- **Source term**

$$l(u, \sigma_{LCR}, \Theta, p)$$

Problem Formulation

- **Set** $X := \left[H_0^1(\Omega)\right]^2 \times \left[L^2(\Omega)\right]^4 \times H^1(\Omega),\ Q := L_0^2(\Omega)$

$$\tilde{u} := (u, \sigma_{LCR}, \Theta) \qquad \tilde{A} := \begin{bmatrix} A & C & 0 \\ \tilde{C}^T & D & 0 \\ E_{fD} & E_{\sigma_{LCR}} & E \end{bmatrix}$$

- **Find** $(\tilde{u}, p) \in X \times Q$ **such that**

$$\left\langle K(\tilde{u}, p), (\tilde{v}, q) \right\rangle = \left\langle l(\tilde{v}, q) \right\rangle \quad \forall (\tilde{v}, q) \in X \times Q$$

$$K = \begin{bmatrix} \tilde{A} & \tilde{B} \\ B^T & 0 \end{bmatrix}$$

(Non-)Classical saddle point problem

- **Compatibility condition**

$$\sup_{u \in \left[H_0^1(\Omega)\right]^2} \frac{\int_\Omega \nabla \cdot u \, q \, dx}{\|u\|_{1,\Omega}} \geq \beta_1 \|q\|_{0,\Omega} \qquad \forall q \in L_0^2(\Omega)$$

$$\sup_{\sigma \in \left[L^2(\Omega)\right]^4} \frac{\int_\Omega \sigma : \nabla u \, dx}{\|\sigma\|_{0,\Omega}} \geq \beta_2 \|u\|_{1,\Omega} \qquad \forall u \in \left[H_0^1(\Omega)\right]^2$$

- **Edge-oriented stabilization for**
  - **Equal order finite element interpolation for velocity and stress**
  - **Convective dominated problem**

$$\left\langle J_{\tilde{u}}\tilde{u},\tilde{v}\right\rangle = \sum_{edgeE} \max\left(\gamma_u \eta_p h_E, \gamma_{\tilde{u}} h_E^2\right)\int_E [\nabla\tilde{u}][\nabla\tilde{v}]ds$$

with $\tilde{u}=(u,\sigma,\Theta)$, $\tilde{v}=(v,\tau,\Phi)$ **and** $[\nabla\tilde{u}][\nabla\tilde{v}]=\sum_i [\nabla\tilde{u}_i][\nabla\tilde{v}_i]$

Then: Efficient Newton-type and multigrid solvers can be „easily“ applied

Nonlinear Solver

- **Damped Newton results in the solution of the form**

$$R(x) = 0, \; x = (u, \sigma_{LCR}, \Theta, p)$$

$$x^{l+1} = x^l + \omega^l \left[\frac{\partial R(x^l)}{\partial x} \right]^{-1} R(x^l)$$

- **Inexact Newton:** Jacobian is approximated using finite differences

$$\left[\frac{\partial R(x^l)}{\partial x} \right]_{ij} \approx \frac{R_j(x + \varepsilon e_i) - R_j(x - \varepsilon e_i)}{2\varepsilon}$$

Jacobian Matrix

- **The Jacobian matrix takes the form**

$$J = \left[\frac{\partial R(x^n)}{\partial x} \right] = \begin{bmatrix} A & \tilde{B}^T \\ B & 0 \end{bmatrix}$$

- **Generalized non-isothermal non-Newtonian problem**

$$A = \begin{bmatrix} A_u & \tilde{C}^T & \tilde{H}^T \\ C & A_\sigma & 0 \\ H & 0 & A_\Theta \end{bmatrix}$$

Modified saddle point problem

Linear Solver

- **Monolithic multigrid solver**

  - **Standard geometric multigrid approach**

  - **Full** Q_2, P_1^{disc} **restrictions and prolongations**

  - **Local MPSC via Vanka-like smoother**

$$\begin{bmatrix} \tilde{u}^{l+1} \\ p^{l+1} \end{bmatrix} = \begin{bmatrix} \tilde{u}^{l} \\ p^{l} \end{bmatrix} + \omega^l \sum_{T \in T_h} \left[J_{|T} \right]^{-1} \begin{bmatrix} R_u(\tilde{u}^l, p^l) \\ R_p(\tilde{u}^l, p^l) \end{bmatrix}_{|T}$$

Fully implicit Monolithic FEM-Multigrid Solver

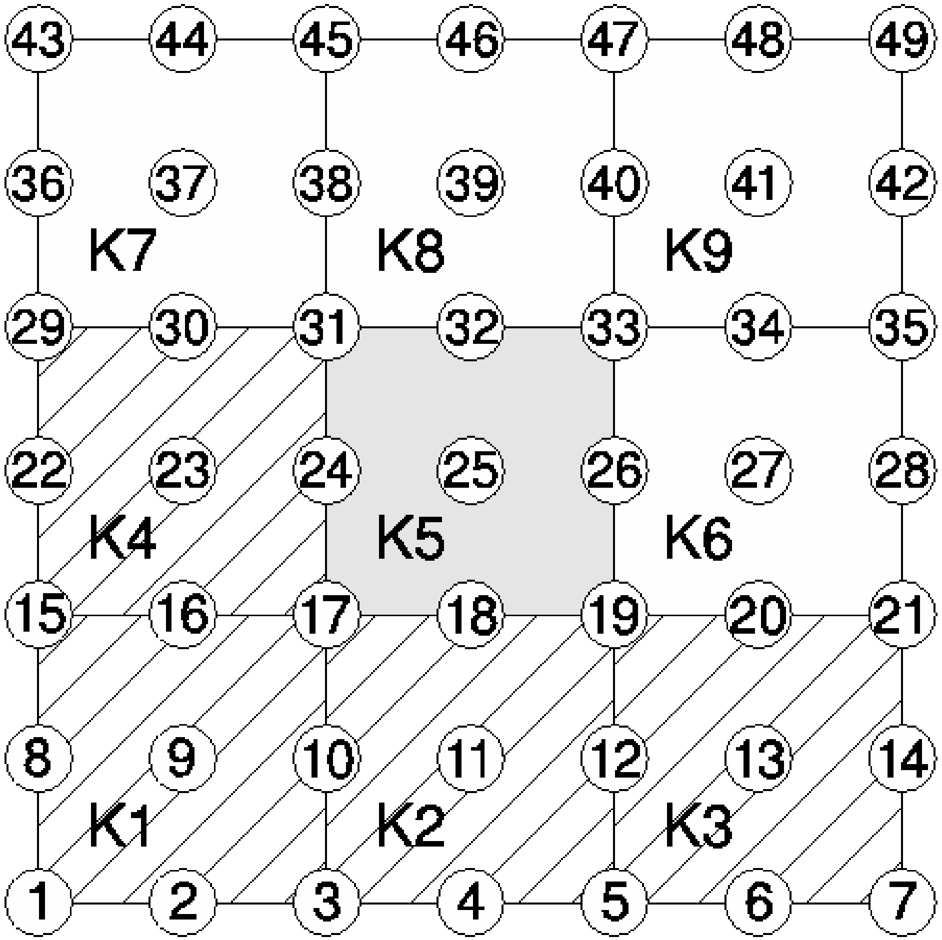

Vanka-like Smoother

Algorithm 1: Smoothing steps

Input: Predefined constant: $\omega > 0$, Number of smoothing steps: NSM

for $j = 1$ **to** NSM **do**
  for $K \in \Omega_h$ **do**
    $x_{I(K)} \leftarrow x_{I(K)} + \omega C_K^{-1}(\mathbf{b} - A\mathbf{x})_{I(K)}$
Return $\mathbf{x}$
end

$$\begin{pmatrix} x_{17} \\ x_{18} \\ x_{19} \\ x_{24} \\ x_{25} \\ x_{26} \\ x_{31} \\ x_{32} \\ x_{33} \end{pmatrix} \leftarrow \begin{pmatrix} x_{17} \\ x_{18} \\ x_{19} \\ x_{24} \\ x_{25} \\ x_{26} \\ x_{31} \\ x_{32} \\ x_{33} \end{pmatrix} + \omega C_5^{-1} \left(\begin{pmatrix} b_1 \\ . \\ . \\ . \\ b_{49} \end{pmatrix} - \begin{pmatrix} a_{1,1} & \cdots & a_{1,49} \\ . & \cdots & . \\ . & \cdots & . \\ . & \cdots & . \\ a_{49,1} & \cdots & a_{49,49} \end{pmatrix} \begin{pmatrix} x_1 \\ . \\ . \\ . \\ x_{49} \end{pmatrix} \right)_{I(K_5)}$$

Dynamic ALE-Mesh Adaptation

Advantages:
- Constant mesh/data structure → **GPU**
- Increased resolution in regions of interest (“r-adaptivity”)
- Anisotropic ‘umbrella’ smoother (with snapping/projection) or GDM
- Straightforward usage on general meshes in 2D / 3D

Quality of the method depends on the construction of the monitor function
- Geometrical description (solid body, interface triangulation)
- Field oriented description (steep gradients, fronts) → numerical stabilization

Validation: 2.5D Rising bubble – light setup

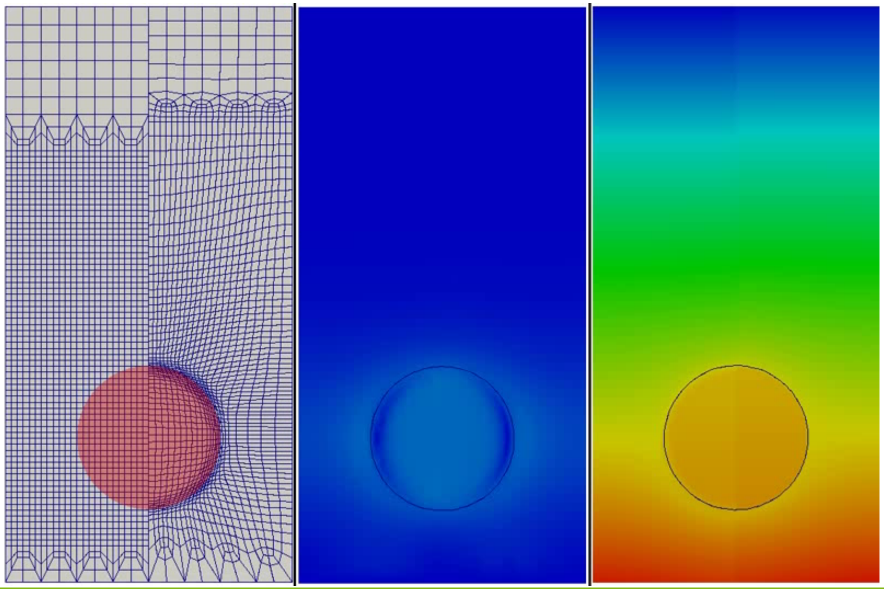

Testing: 3D Rising bubble - hard setup

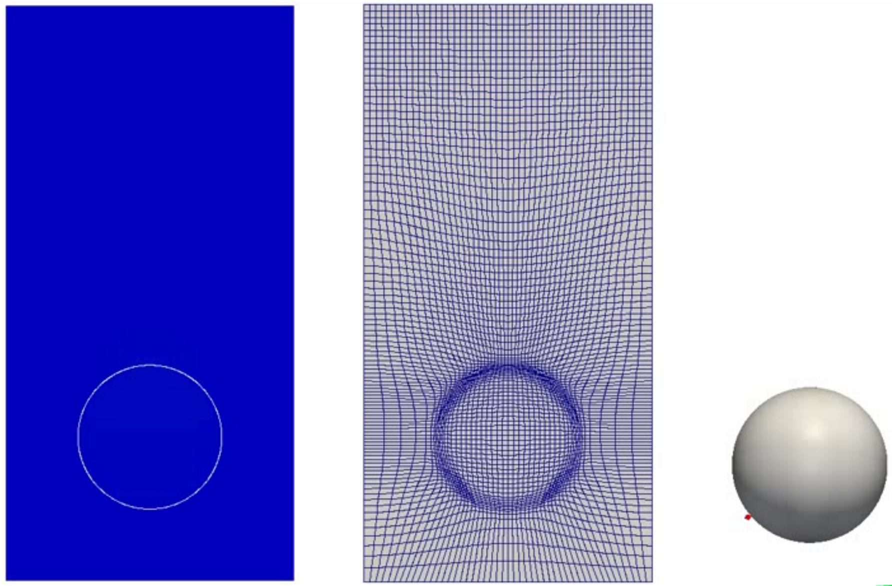

Test: Oscillating Cylinder

- Measure Drag/Lift Coefficients for a sinusoidally oscillating cylinder
- Compare results for FBM, adapted FBM and adapted FBM + boundary projection/parametrization

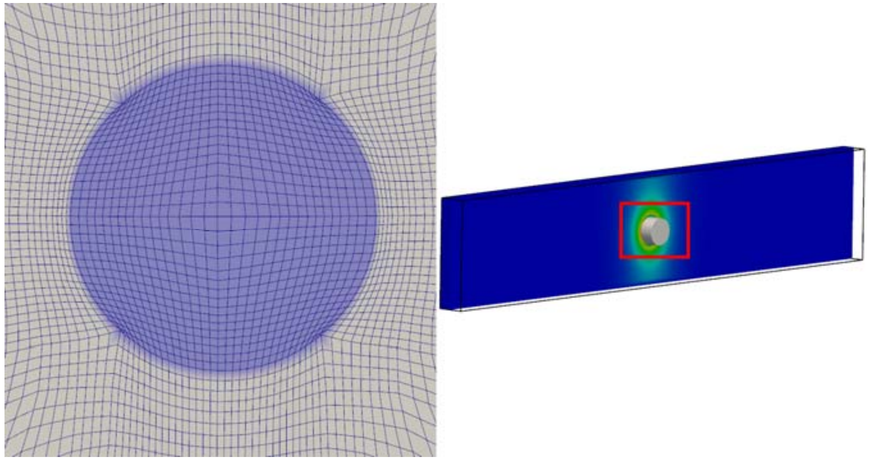

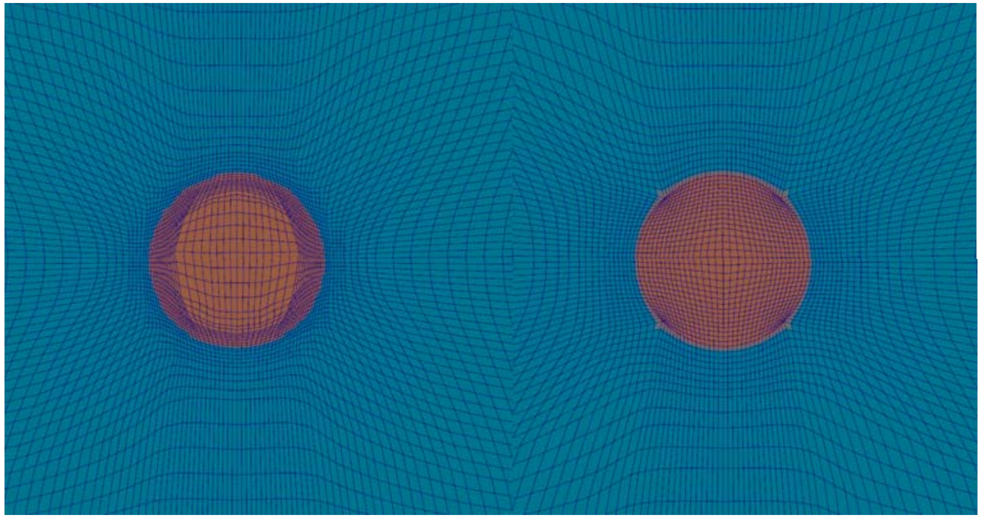

Nodes concentrated near liquid-solid interface

Nodes projected and parametrized on boundary plus concentration of nodes near boundary

Oscillating Cylinder Results

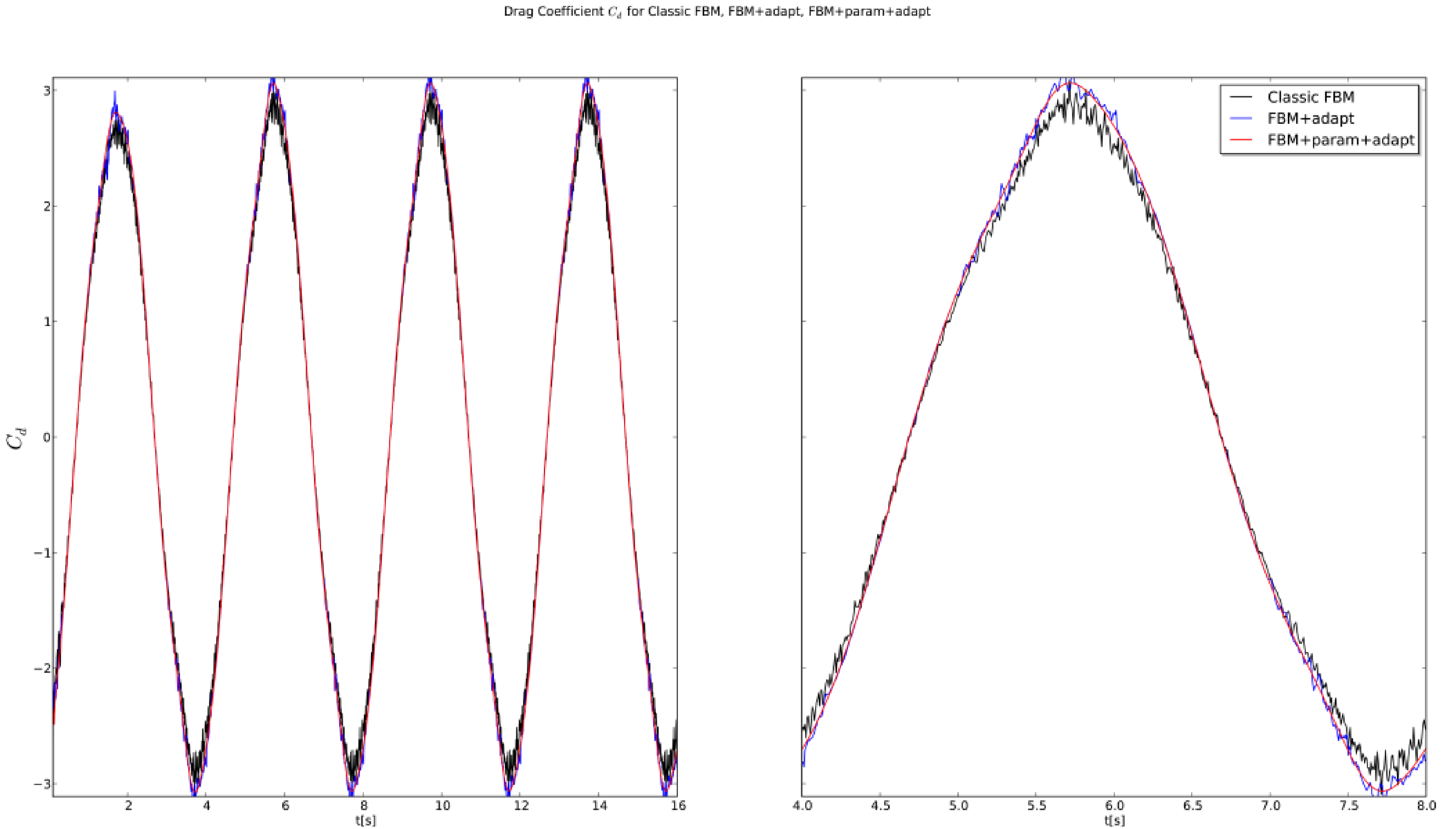

Oscillating Cylinder Results

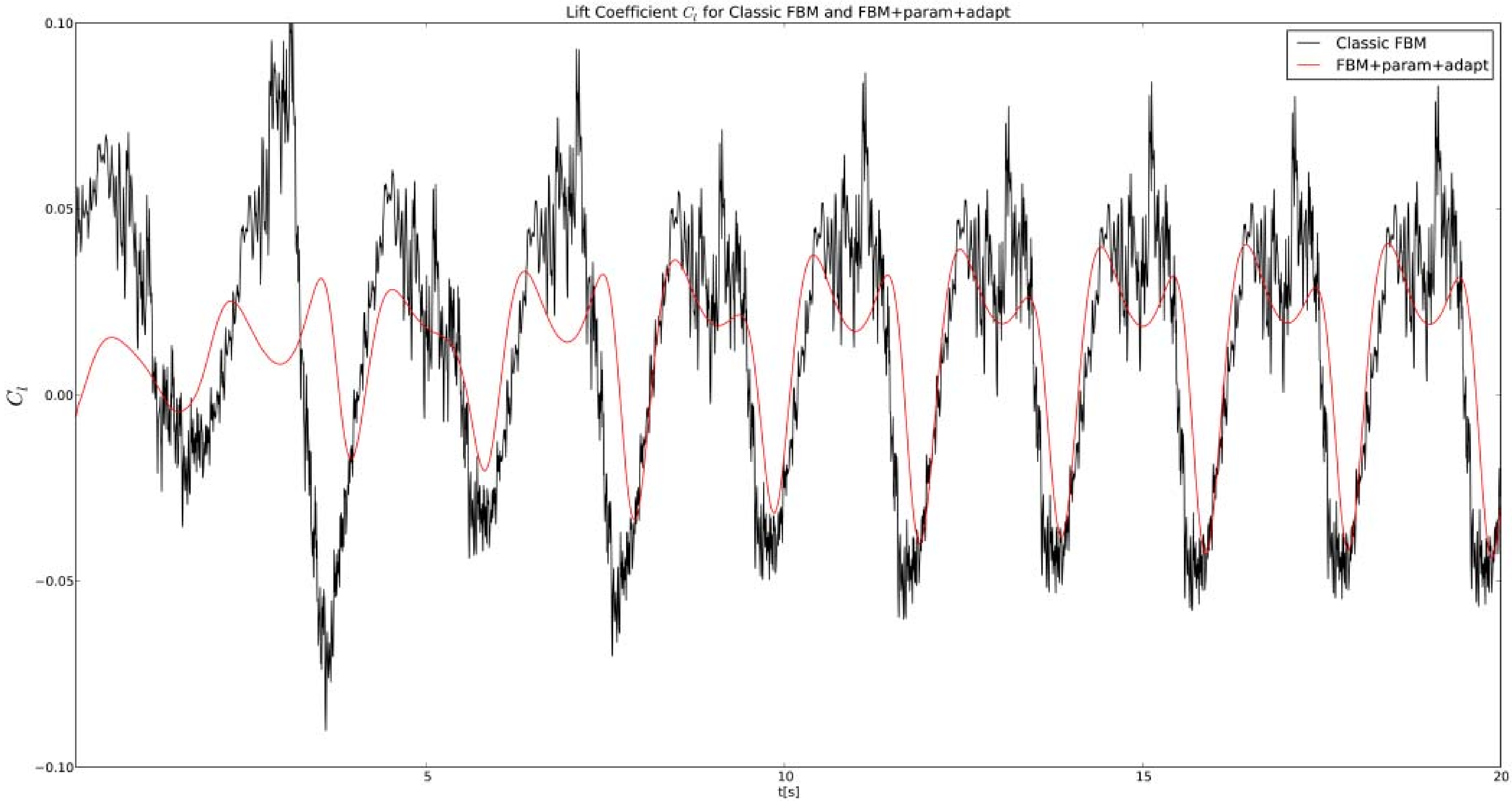

(Passive) Microswimmer

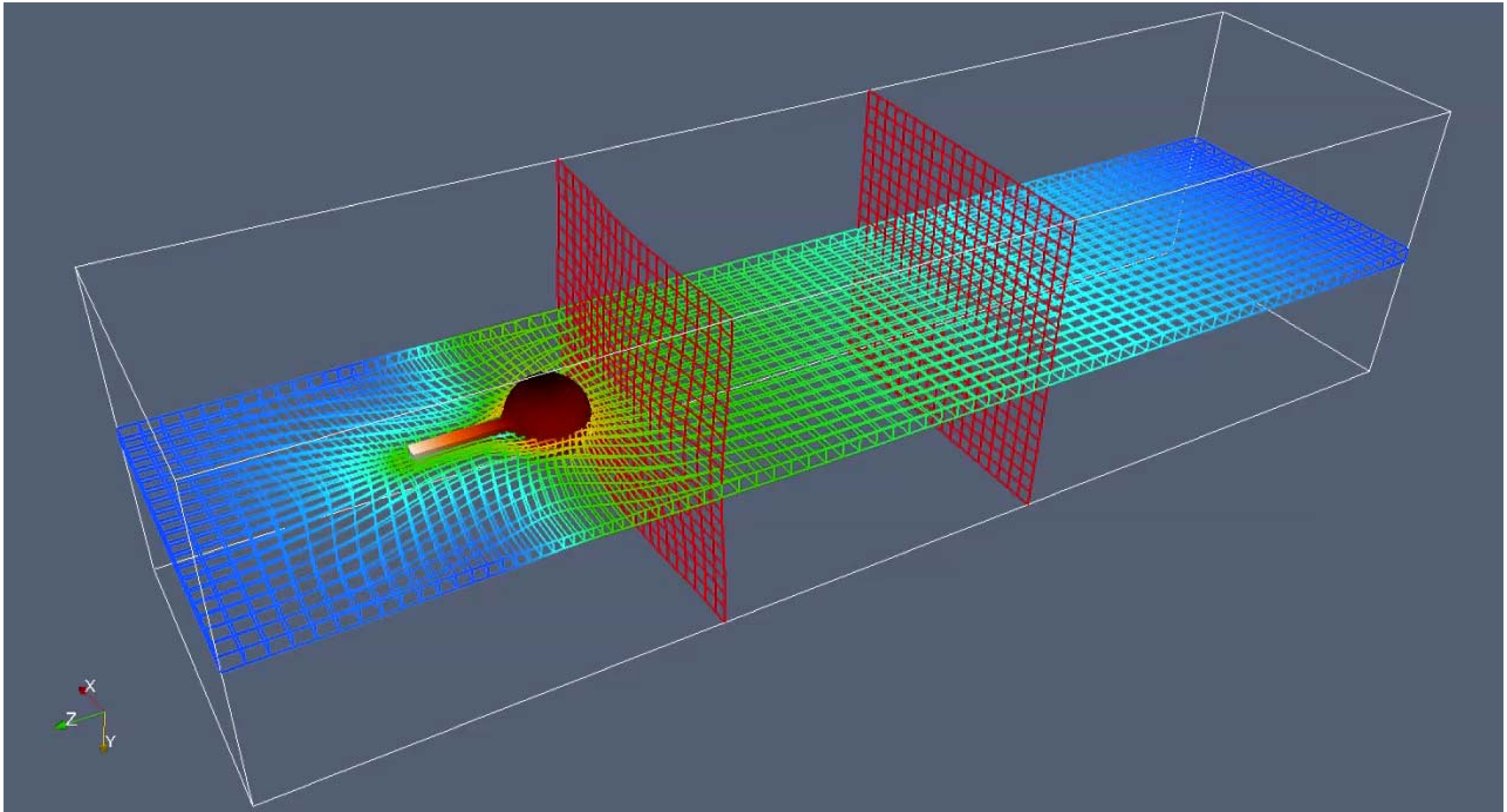

Sedimentation

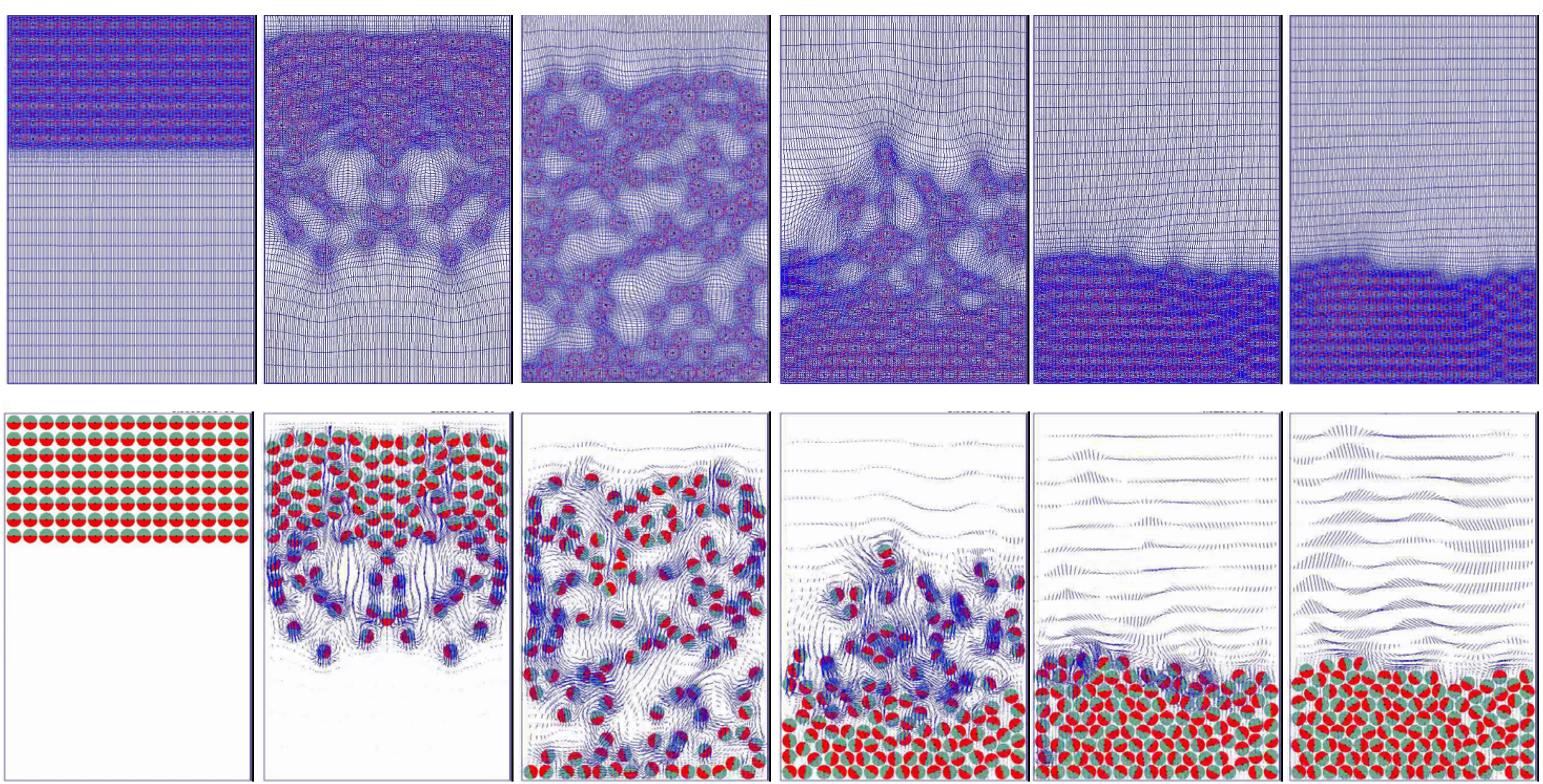

Viscous Liquid Jets

J. M. Nóbrega et al.: The phenomenon of jet buckling: Experimental and numerical predictions

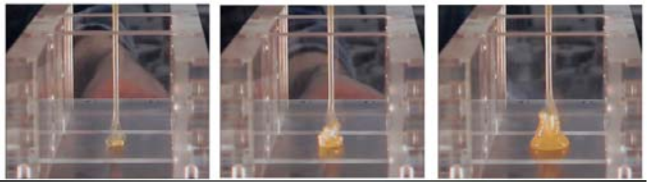

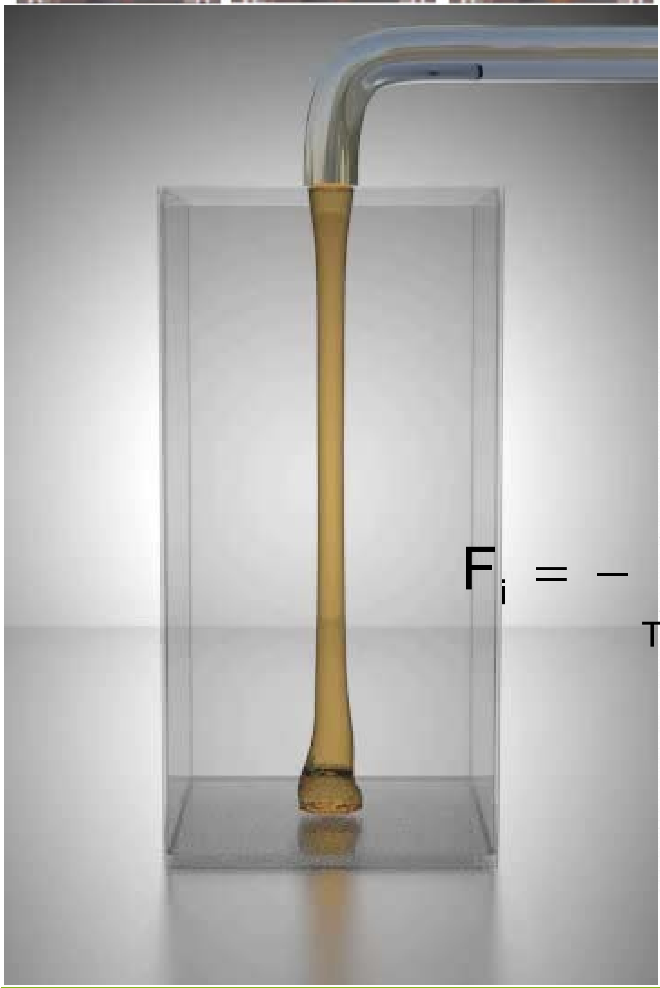

Corn syrup-air system

24x24x48 mesh

Interface triangulation:
T_0: ~100,000 triangles
T_N: ~300,000 triangles

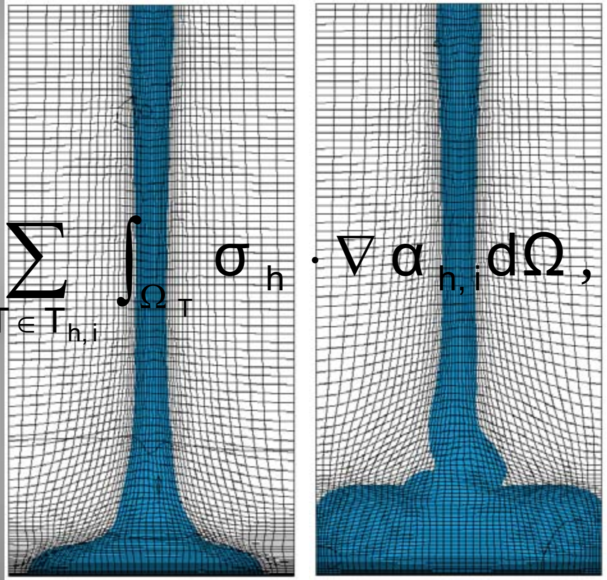

$$F_i = -\sum_{T \in T_{h,i}} \int_{\Omega_T} \sigma_h \cdot \nabla \alpha_{h,i} \, d\Omega ,$$

Rendering: Raphael Münster / Blender

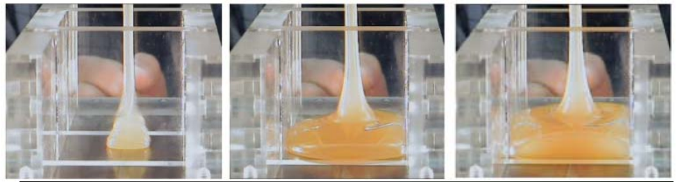

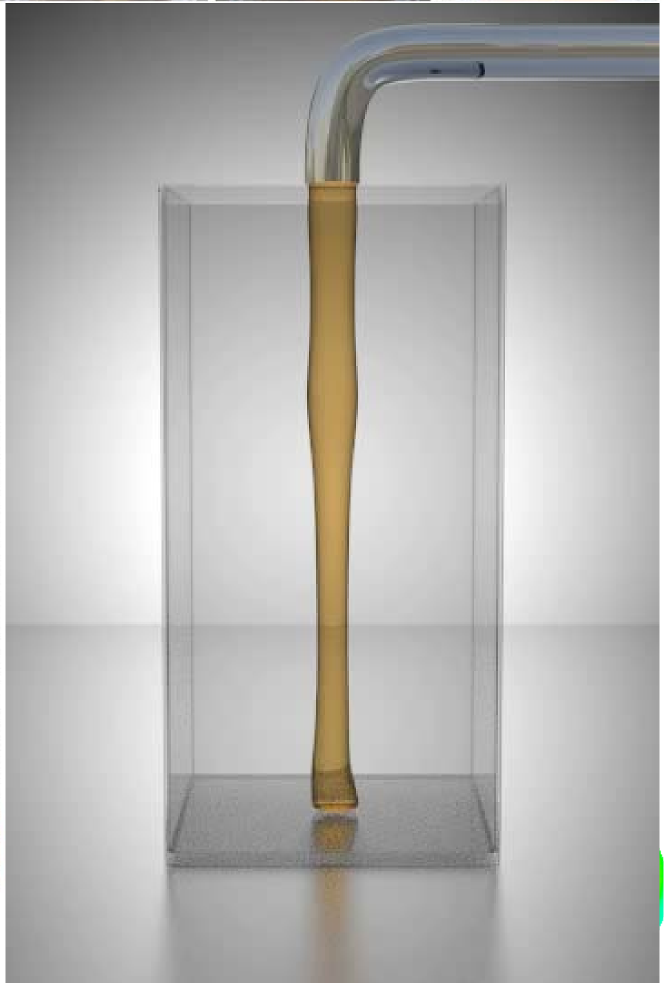

Benchmark Problem

- **Coarse grid and mesh information**

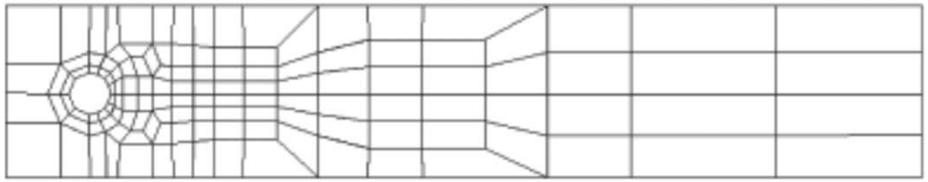

Level	NEL	NMT	NMP
1	520	572	1092
2	2080	2184	4264
3	8320	8528	16848
4	33280	33696	66976
5	133120	133952	267072

- **n.o.f. for different problems**

Level	n.o.f. u	n.o.f p	n.o.f. T	n.o.f S	VP	VPT	VSP
0	1144	390	572	1716	1534	2106	3250
1	4368	1560	2184	6552	5928	8112	12489
2	17056	6240	8528	25584	23296	31824	48880
3	67392	24960	33696	101088	92352	126048	193449
4	267904	99840	133952	401856	367744	501696	769600
5	1068288	399360	534144	1602432	1467648	2001792	3070080

Newtonian Problem (VP)

Stokes

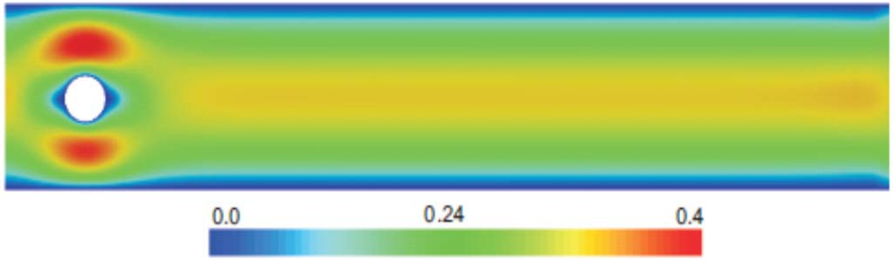

Navier-Stokes Re=20

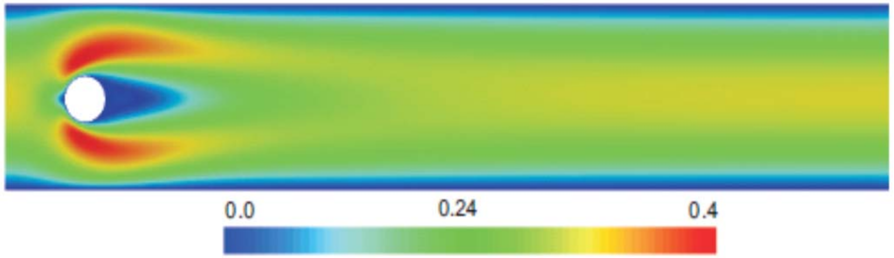

Level	Drag	Lift	N/L	Drag	Lift	N/L
1	3.112646	2.965870e-2	1/6	5.540999	9.447473e-3	5/2
2	3.134342	3.005275e-2	1/7	5.566928	1.046885e-2	5/2
3	3.140327	3.015909e-2	1/7	5.576088	1.056787e-2	5/2
4	3.141893	3.018665e-2	1/7	5.578652	1.060398e-2	5/2
5	3.142292	3.019366e-2	1/7	5.579313	1.061503e-2	5/2

Level independent solver

Power Law Problem (VP)

technische universität dortmund

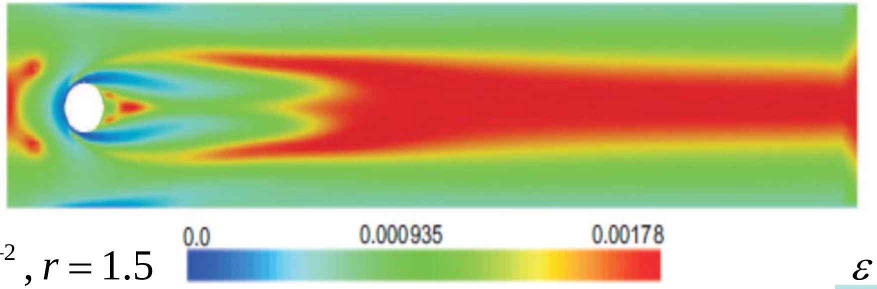

$$\eta_s(\dot\gamma,\Theta,p)=\eta_0(\varepsilon+\dot\gamma^2)^{(\frac{r}{2}-1)},(\eta_0>0,r>1).$$

$\varepsilon=10^{-2}, r=1.5$

Level	Drag	Lift	N/L
2	3.26420	-0.01339	4/2
3	3.27728	-0.01341	3/2
4	3.27956	-0.01338	2/2
5	3.28007	-0.01337	2/2

$\varepsilon=10^{-2}, r=3$

Level	Drag	Lift	N/L
2	13.74280	0.35070	3/2
3	13.77355	0.34963	3/2
4	13.78220	0.35062	3/1
5	13.78445	0.35112	2/2

$\varepsilon=10^{-4}, r=1.5$

Level	Drag	Lift	N/L
2	3.26433	-0.01342	4/2
3	3.27739	-0.01342	3/2
4	3.27968	-0.01339	2/2
5	3.28019	-0.01338	2/2

$\varepsilon=10^{-4}, r=3$

Level	Drag	Lift	N/L
2	13.73800	0.35052	3/2
3	13.76875	0.34941	3/2
4	13.77740	0.35040	3/1
5	13.77970	0.35091	2/2

Level and parameter independent solver

Cross Model Problem (VP)

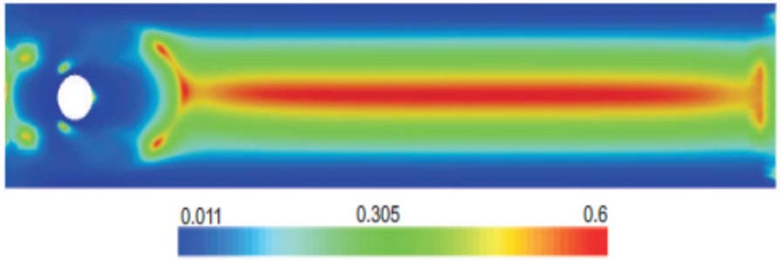

$$\eta_s(\dot\gamma,\Theta,p)=\eta_\infty+\frac{(\eta_0-\eta_\infty)}{(1+(\lambda\dot\gamma)^{r_1})^r}\exp(\alpha p+(a_1+\frac{a_2}{a_3+\Theta})),$$

$\eta_\infty=10^{-3},\ a_1=a_2=0,$

$r=1,\ r_1=1,\ \alpha=0,\ \eta_0=10^{-2}$

Level	Drag	Lift	N/L
2	6.31313	0.02478	3/1
3	6.32337	0.02504	3/2
4	6.32619	0.02509	3/2
5	6.32691	0.02510	2/2

$r=0,\ r_1=1,\ \alpha=0.1,\ \eta_0=10^{-1}$

Level	Drag	Lift	N/L
2	534.29750	6.53247	3/2
3	535.48500	6.55813	3/3
4	535.77950	6.56464	3/3
5	535.84800	6.56621	2/2

$r=0,\ r_1=1,\ \alpha=0.1,\ \eta_0=10^{-2}$

Level	Drag	Lift	N/L
2	33.22763	0.81901	2/2
3	33.29026	0.82140	2/2
4	33.30657	0.82201	2/2
5	33.31069	0.82217	2/2

$r=1,\ r_1=1,\ \alpha=0.1,\ \eta_0=10^{-1}$

Level	Drag	Lift	N/L
2	15.16395	0.13886	4/3
3	15.18516	0.13963	4/3
4	15.19108	0.13978	4/3
5	15.19262	0.13982	3/3

Level and model independent solver

Cross Model problem (VTP)

technische universität dortmund

Non heated cylinder

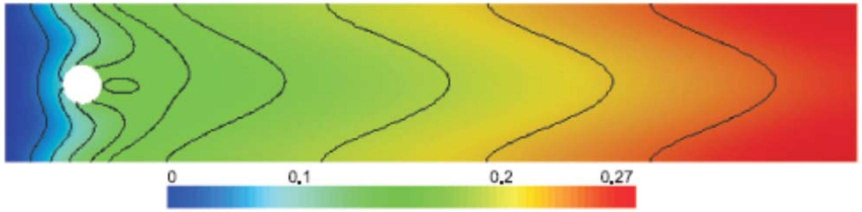

$$\eta_s(\dot{\gamma},\Theta,p)=\eta_\infty+\frac{(\eta_0-\eta_\infty)}{(1+(\lambda\dot{\gamma})^{r_1})^r}\exp(\alpha p+(a_1+\frac{a_2}{a_3+\Theta})),$$

$$\eta_\infty=10^{-3}, a_1=0,\ a_3=1,\ k_1=k_2=10^{-2},$$

$r=0,\ r_1=1,\ \alpha=0,\ \eta_0=10^{-2},\ a_2=0.$

Level	Drag	Lift	N/L
2	74.29465	1.31636	2/2
3	74.43290	1.32009	2/2
4	74.46910	1.32105	2/2
5	74.47830	1.32129	2/2

$r=0.1,\ r_1=1,\ \alpha=0, \eta_0=10^{-1},\ a_2=0.$

Level	Drag	Lift	N/L
2	5579.355	54.79350	3/2
3	5589.415	54.96815	3/3
4	5592.050	55.01415	3/3
5	5592.725	55.02585	3/2

$r=0.1,\ r_1=1,\ \alpha=0,\ \eta_0=10^{-2},\ a_2=1.$

Level	Drag	Lift	N/L
2	53.78930	1.05488	2/2
3	53.88590	1.05770	3/2
4	53.91125	1.05844	2/2
5	53.91770	1.05863	2/2

$r=0.1,\ r_1=1,\ \alpha=10^{-3},\ \eta_0=10^{-1},\ a_2=1.$

Level	Drag	Lift	N/L
2	6005.265	59.75125	3/2
3	6016.220	59.94455	3/2
4	6019.075	59.99535	3/2
5	6019.795	60.00820	3/2

Level and model independent solver

Cross Model Problem (VTP)

Heated cylinder

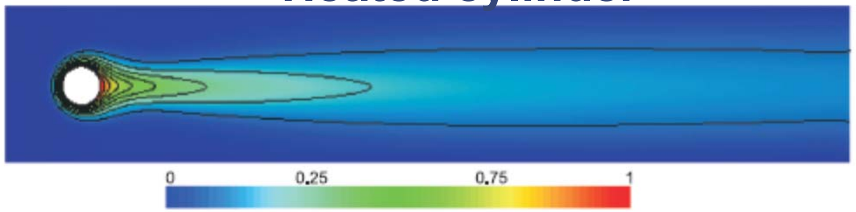

$$\eta_s(\dot\gamma,\Theta,p)=\eta_\infty+\frac{(\eta_0-\eta_\infty)}{(1+(\lambda\dot\gamma)^{r_1})^r}\exp(\alpha p+(a_1+\frac{a_2}{a_3+\Theta})),$$

$\eta_\infty=10^{-3}, r=0.1, r_1=1, \alpha=10^{-3}, a_1=0, a_2=1, a_3=1,$

$\eta_0=10^{-2},\ k_1=k_2=10^{-2}.$

Level	Drag	Lift	N/L
2	45.26969	0.90303	3/2
3	45.35251	0.90563	3/2
4	45.37431	0.90632	2/2
5	45.37988	0.90649	2/2

$\eta_0=10^{-1},\ k_1=k_2=10^{-3}.$

Level	Drag	Lift	N/L
2	512.7765	5.37640	3/2
3	513.7120	5.39301	3/3
4	513.9585	5.39743	3/3
5	514.0215	5.39856	3/2

$\eta_0=10^{-1},\ k_1=k_2=10^{-2}.$

Level	Drag	Lift	N/L
2	464.07865	4.90752	2/2
3	464.93045	4.92313	3/2
4	465.15470	4.92724	2/2
5	465.21195	4.92828	2/2

$\eta_0=1.0,\ k_1=k_2=10^{-3}.$

Level	Drag	Lift	N/L
2	5528.860	53.11685	3/2
3	5539.025	53.28790	3/2
4	5541.690	53.33335	3/2
5	5542.365	53.34490	3/2

Level and model independent solver

Barus Model Problem (VP)

- **Coarse grid and mesh information**

Mesh1

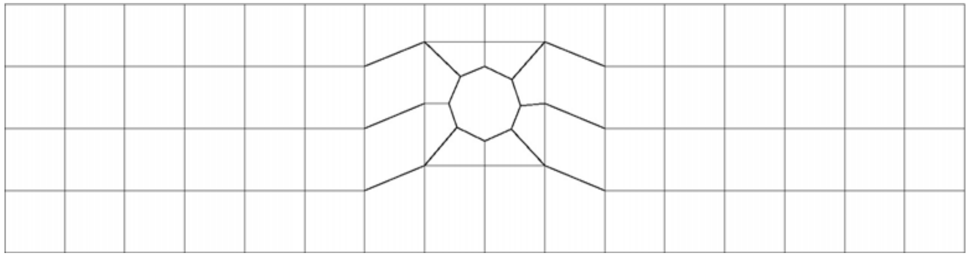

Mesh2

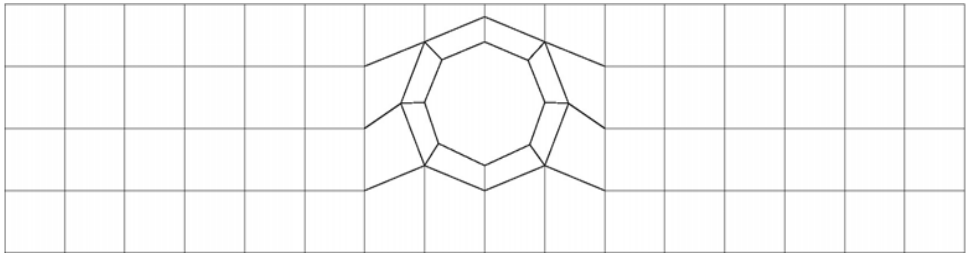

Mesh3

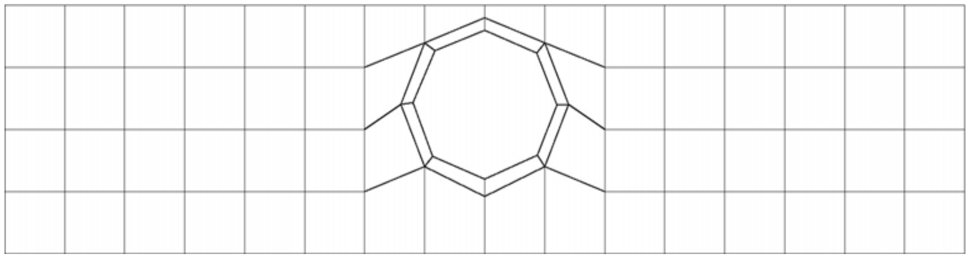

Level	NEL	NMT
1	68	160
2	272	592
3	1088	2272
4	4352	8896
5	17408	35200

$$\eta_S(\dot{\gamma}, \Theta, p) = \eta_0 \exp^{\alpha p}$$

$$\eta_0 = 0.105$$

$$\alpha = 0.1$$

Barus Model Problem (VP)

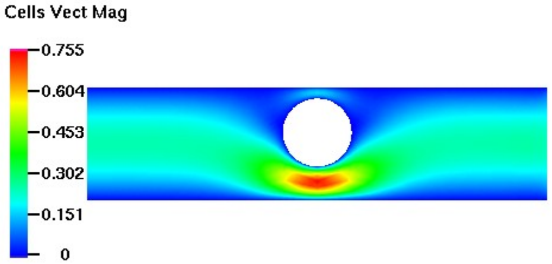

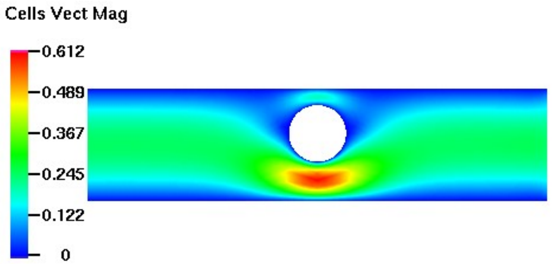

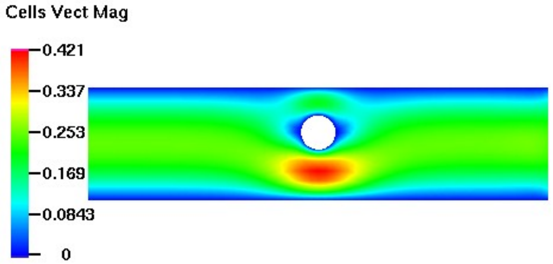

Mesh1, $r = 0.15$

Level	Drag	Lift	N/L
2	1.700913e2	-6.155597	5/2
3	1.721632e2	-6.215218	5/2
4	1.725257e2	-6.228167	4/2
5	1.725743e2	-6.230978	4/2

Mesh2, $r = 0.25$

Level	Drag	Lift	N/L
2	4.802439e2	-1.824015	6/2
3	5.186006e2	-2.106716	6/2
4	5.309640e2	-2.173021	5/2
5	5.354556e2	-2.194828	5/2

Mesh3, $r = 0.30$

Level	Drag	Lift	N/L
2	1.025332e3	-4.720981e1	8/2
3	1.056778e3	-4.945528e1	7/2
4	1.066600e3	-5.012865e1	6/3
5	1.069325e3	-5.032015e1	6/3

Level and parameter independent solver

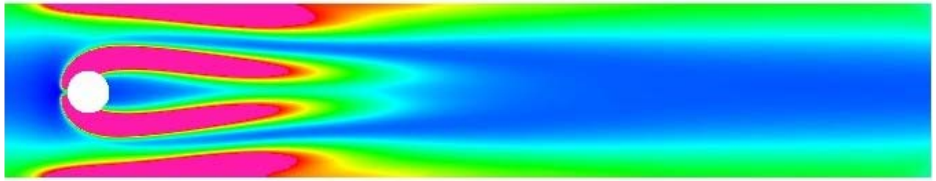

$We = 0.002$ **Oldroyd-B**

Level	Drag	Lift	N/L
2	5.57150	0.01031	2/2
3	5.58032	0.01047	3/2
4	5.58285	0.01051	2/2
5	5.58351	0.01052	2/2

$We = 0.002$ **Giesekus**

Level	Drag	Lift	N/L
2	5.56474	0.01053	2/2
3	5.57511	0.01064	2/2
4	5.57936	0.01062	2/2
5	5.58131	0.01059	2/2

$We = 1.0$ **Oldroyd-B**

Level	Drag	Lift	N/L
2	20.8412	0.32761	7/7
3	17.7123	0.22910	6/8
4	15.0096	0.14311	6/9
5	12.58895	0.07002	6/9

$We = 1.0$ **Giesekus**

Level	Drag	Lift	N/L
2	5.03961	-0.00172	4/2
3	4.93834	-0.00210	4/3
4	4.84483	-0.00252	3/3
5	4.77541	-0.00276	3/4

Level independent solver

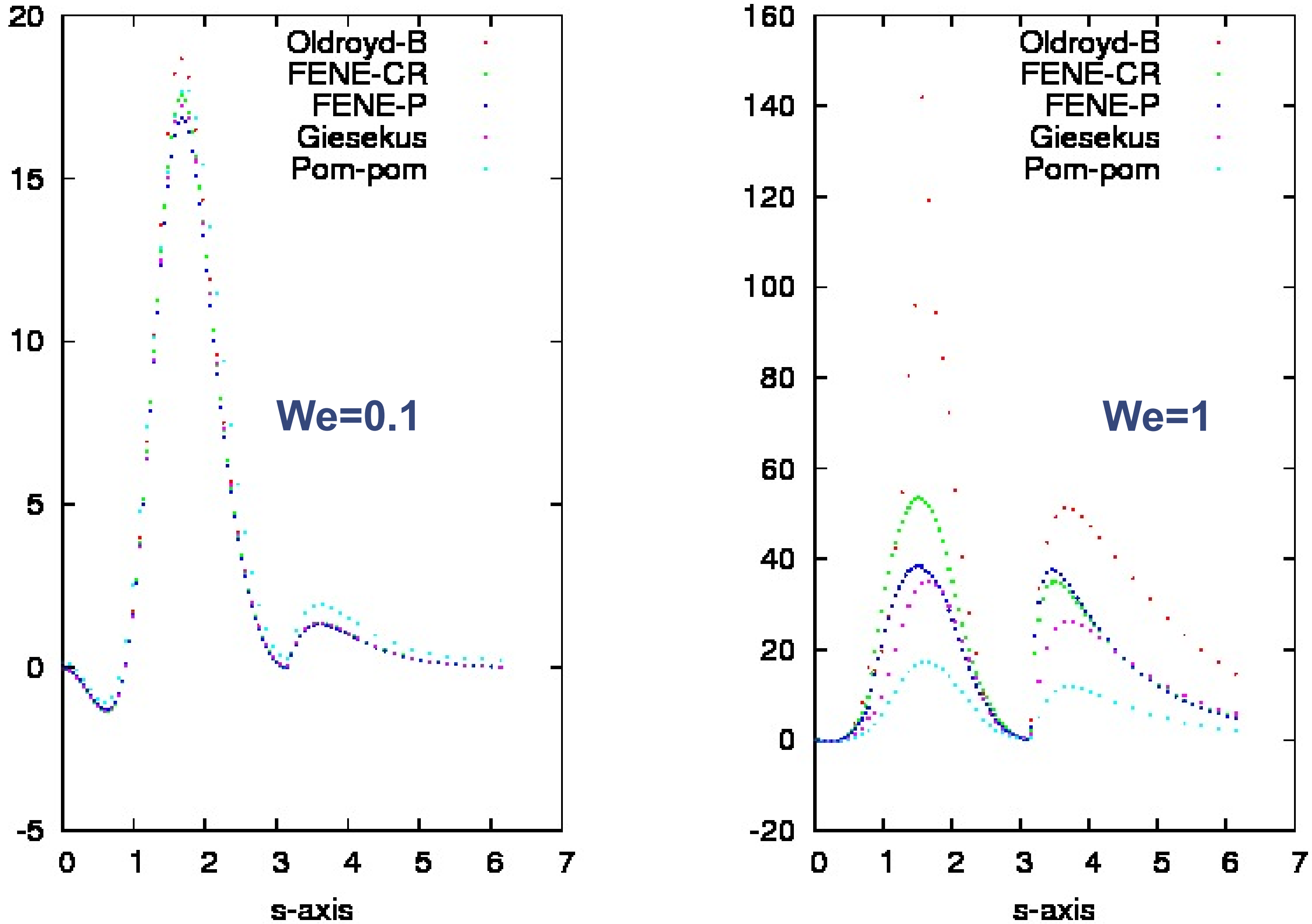

Lower We vs. higher We

Viscoelastic Fluids (VSP)

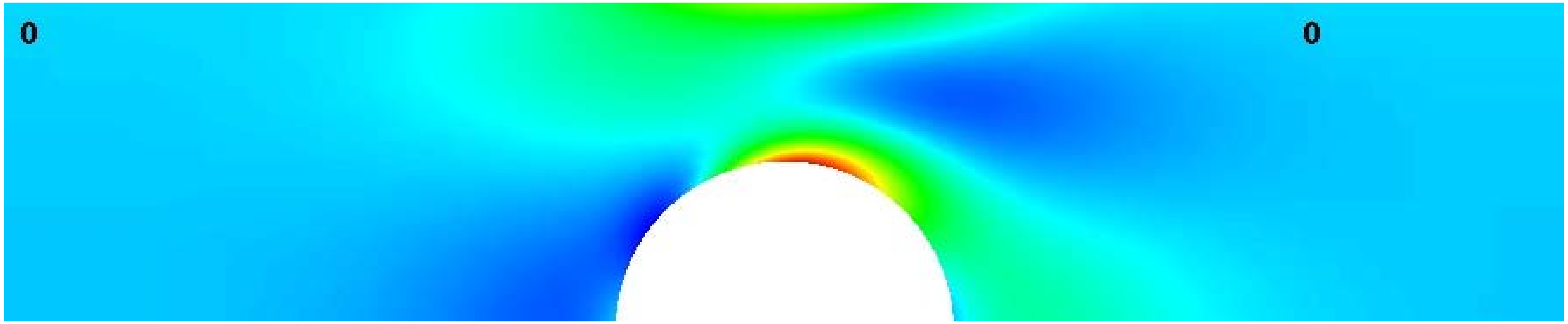

We	0.1	0.2	0.3	0.4	0.5	0.6	…	1.0
Oldroyd-B	5 [130.06]	4 [130.06]	4 [130.06]	5 [120.40]	5 [118.67]	5 [117.66]	…	7 [119.33]
Giesekus	4 [129.37]	4 [124.41]	4 [119.86]	3 [116.31]	3 [113.67]	3 [111.71]	…	3 [107.29]
Fene-P	4 [128.91]	4 [124.62]	4 [120.70]	3 [117.67]	3 [115.51]	4 [114.02]	…	3 [111.84]
Fene-CR	4 [130.15]	4 [126.72]	4 [123.68]	3 [121.51]	3 [120.14]	3 [119.42]	…	3 [120.13]
Pom-pom	3 [137.17]	4 [127.23]	4 [119.78]	4 [114.51]	4 [110.66]	5 [107.76]	…	3 [101.00]

Lower We vs. higher We

Coarse grid and mesh information

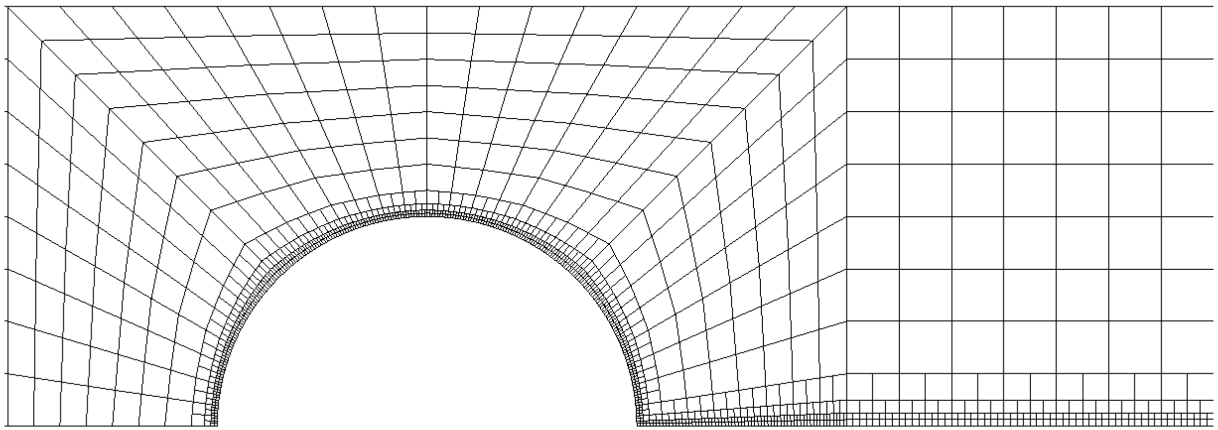

Level	NEL	DOF
R3a1	656	15823
R3a2	944	22457
R3a3	1520	35715
R3a4	2672	62221
R3a5	4976	115223

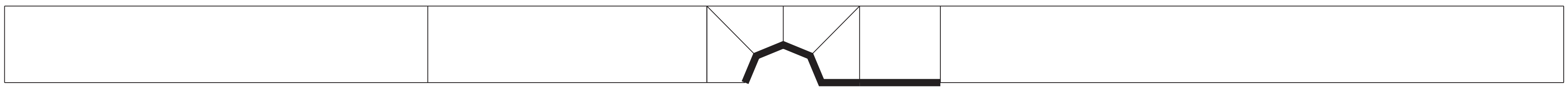

Local refinement via hanging nodes

- **Planar flow around cylinder (Oldroyd-B)**

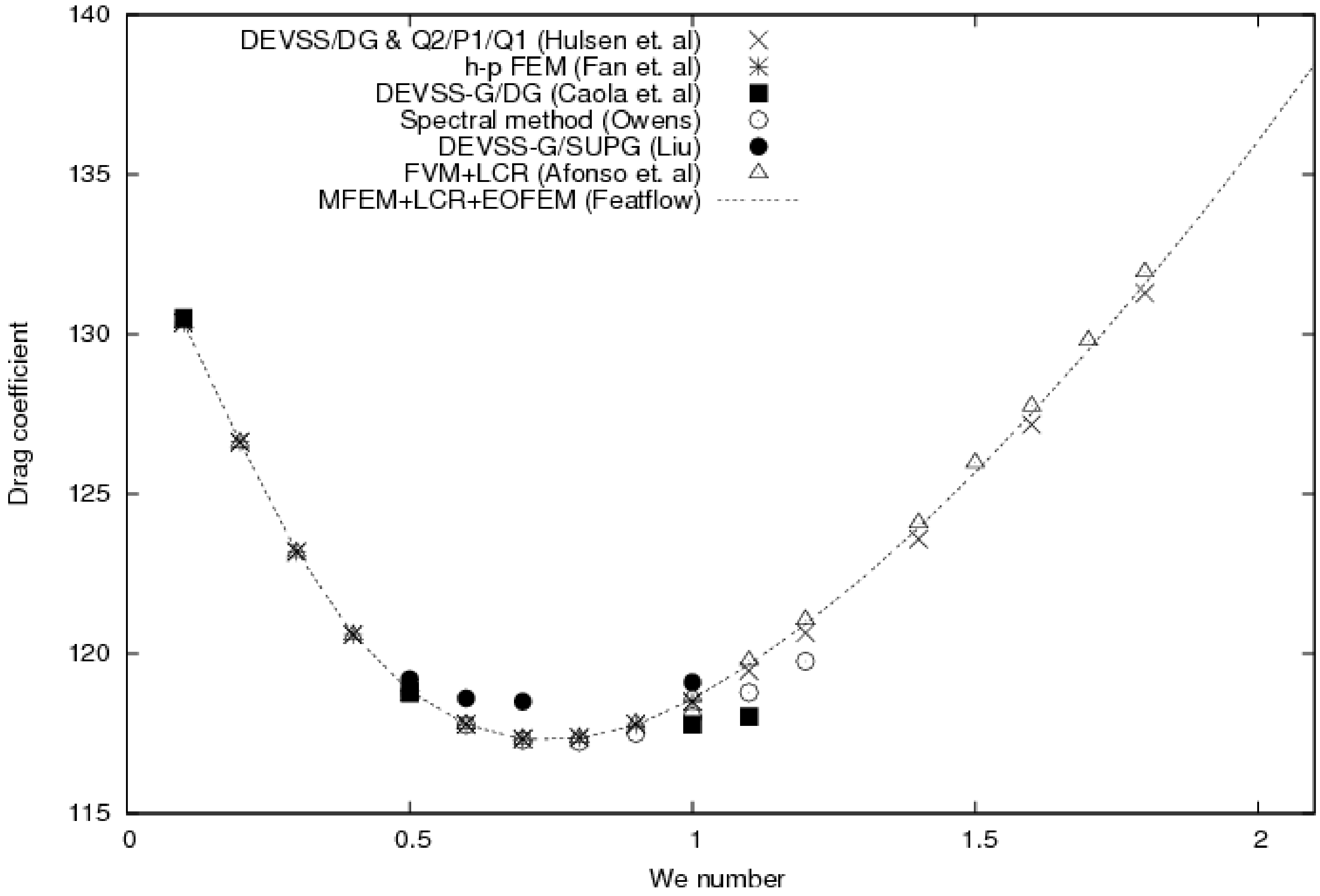

- **Oldroyd-B**

We	Drag	NL	We	Drag	NL	We	Drag	NL
0.1	130.366	8	0.8	117.347	4	1.5	125.665	4
0.3	123.194	4	1.0	118.574	6	1.7	129.494	4
0.5	118.828	4	1.2	120.919	5	1.9	133.754	4
0.6	117.779	4	1.3	122.350	4	2.0	136.039	5
0.7	117.321	4	1.4	123.936	4	2.1	138.438	5

- **Giesekus**

We	Drag	Peak2	NL	We	Drag	Peak2	NL
5	96.943	924.45	14	60	85.859	12010.57	4
20	89.905	4204.51	12	70	85.365	13773.61	4
30	88.304	6318.79	5	80	84.937	15502.45	4
40	87.256	8311.32	5	90	84.585	17207.87	4
50	86.476	10199.1	4	100	84.287	18897.95	4

Efficient continuation for increasing We numbers

Flow around Cylinder Benchmark

- **Direct steady vs. non-steady approach for Giesekus**

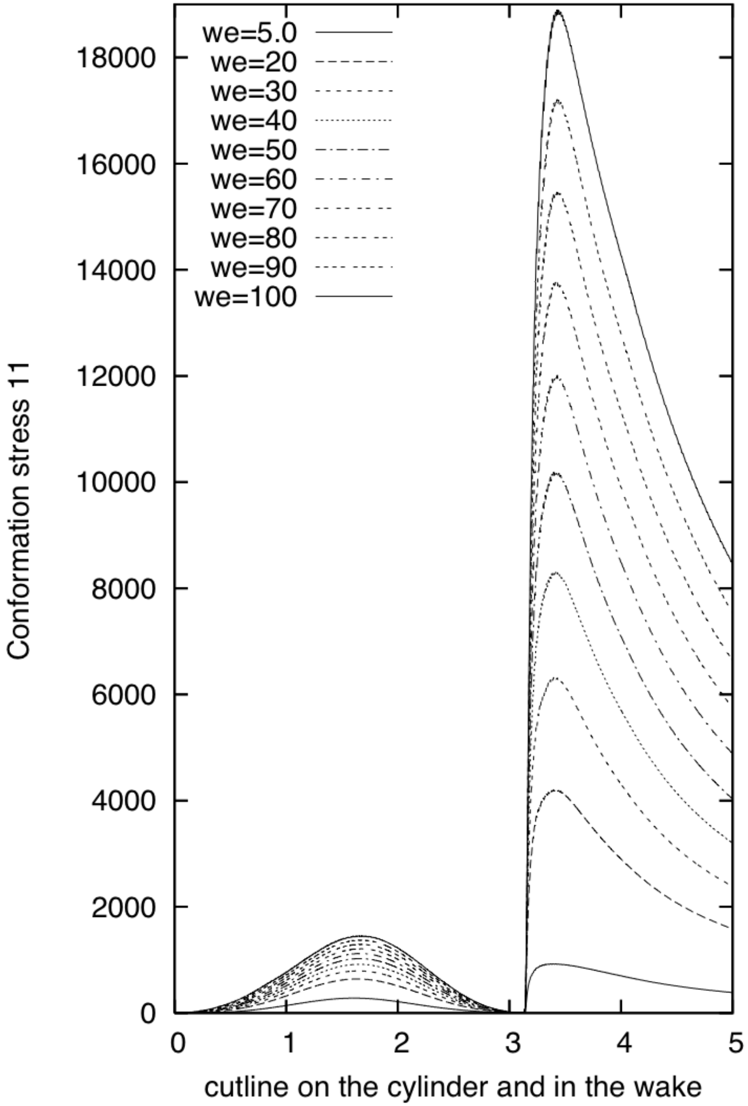

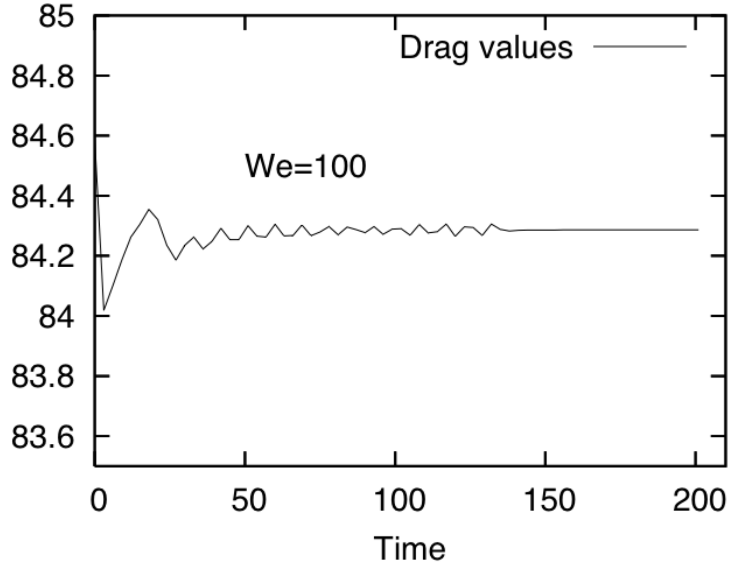

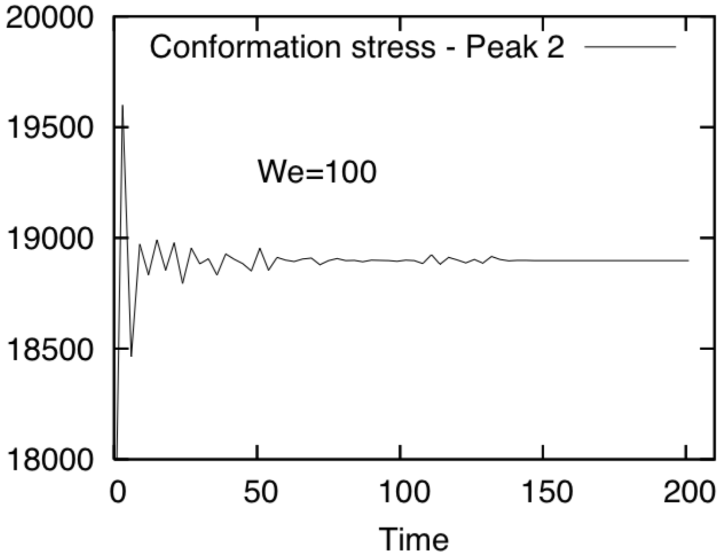

Flow around Cylinder Benchmark

- **Axial stress w.r.t. X-curved: Oldroyd-B vs. Giesekus**

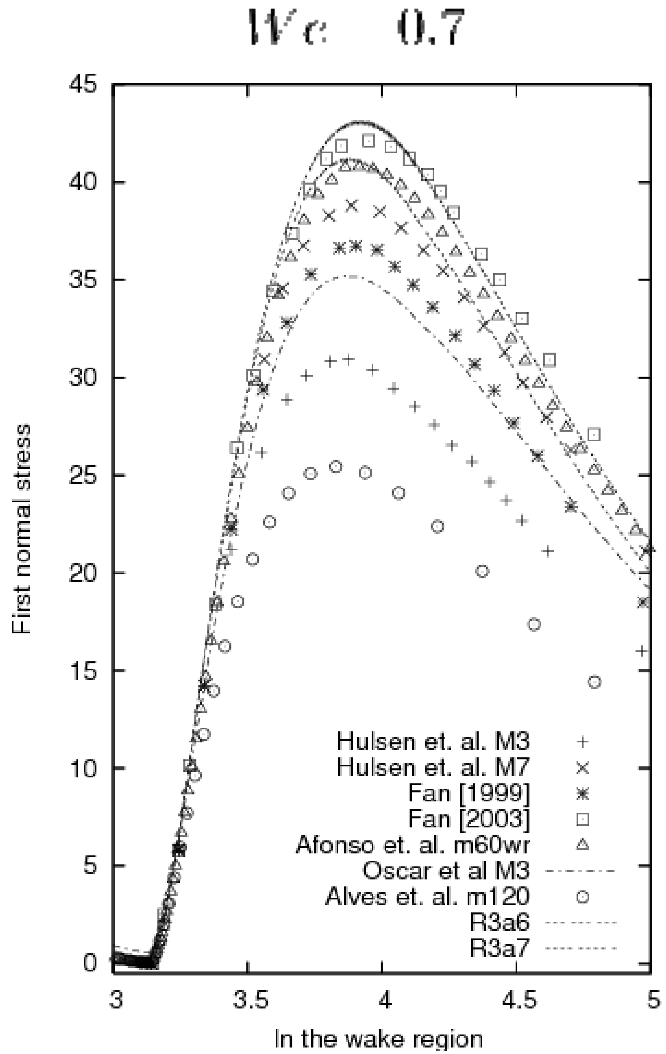

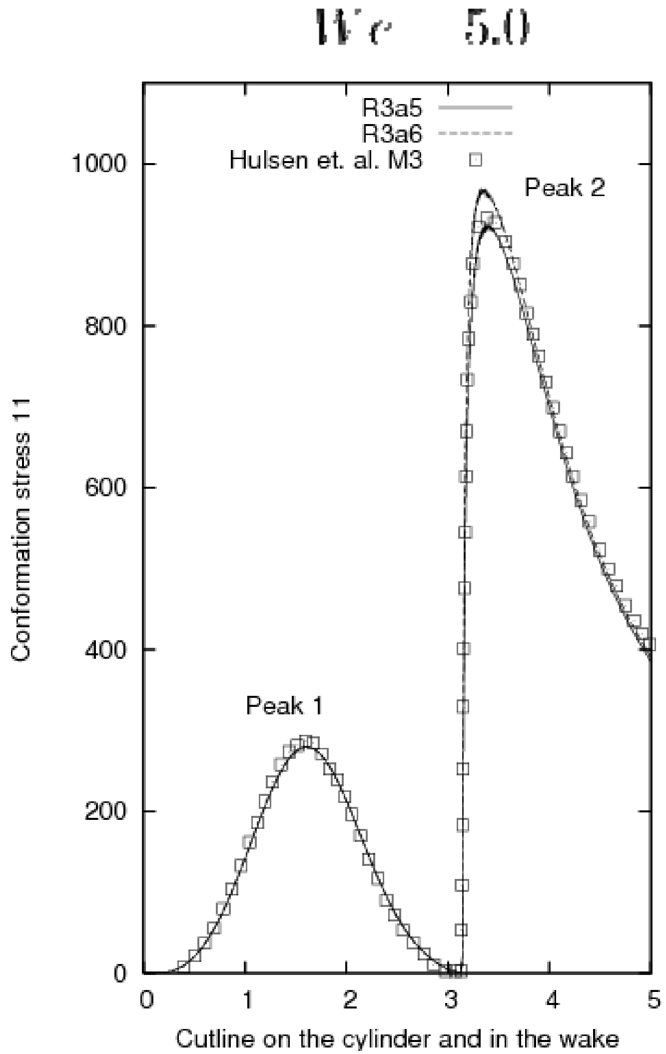

Lack of pointwise mesh convergence due to model (?)

Flow past a sphere benchmark: R.G. Owens T. N. Phillips

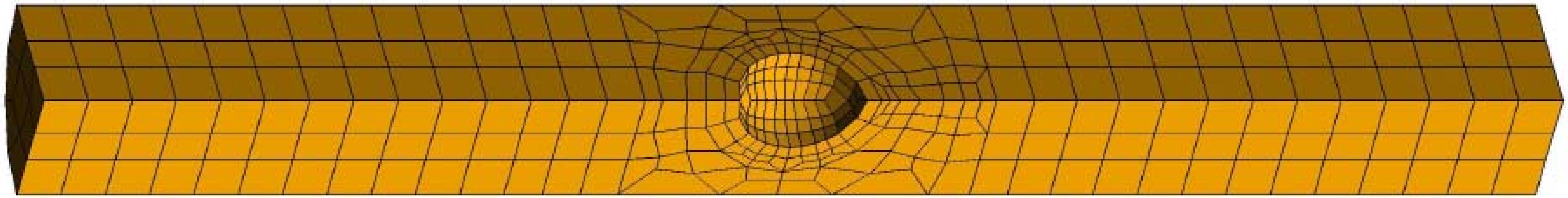

We=0.3

Resolution	$\max_1(\tau_{xx})$	$\max_2(\tau_{xx})$	F^*
L2	20.80	2.082	5.6976
L3	19.29	2.081	5.6946
L4	18.72	2.086	5.6941
L5	18.52	2.087	5.6940
Authors		Reference values	
Lunsmann [4]	-	-	5.6937
Owens [5]	18.27	-	5.6963

We=0.6

Resolution	$\max_1(\tau_{xx})$	$\max_2(\tau_{xx})$	F^*
L2	50.31	5.041	5.4170
L3	39.01	5.061	5.4133
L4	36.43	5.104	5.4128
L5	35.65	5.118	5.4128
Authors		Reference values	
Lunsmann [4]	35.17	-	5.4123
Owens [5]	35.67	-	5.4117
Sahin [6]	34.73	5.12	-

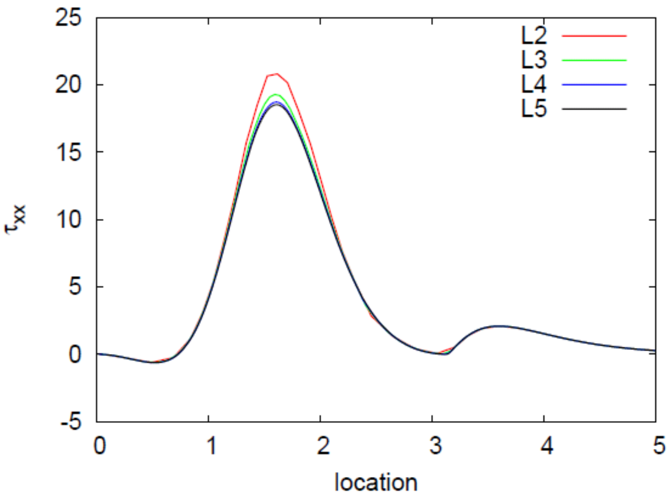

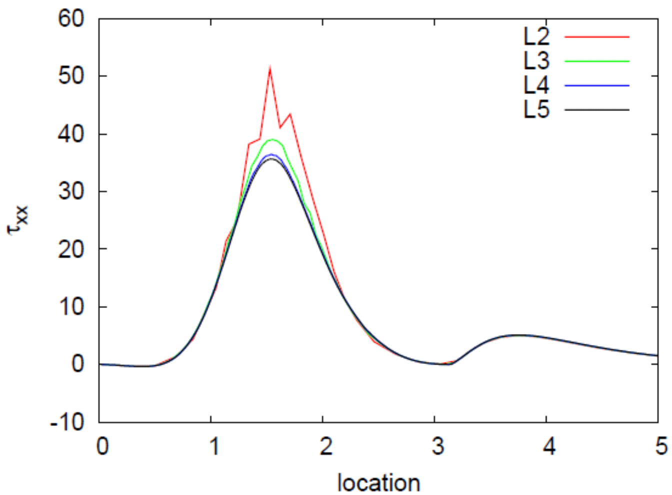

M. Sahin: 3D flow past a cylinder benchmark

Prediction of special viscoelastic flow features for increased We numbers

We=1.2

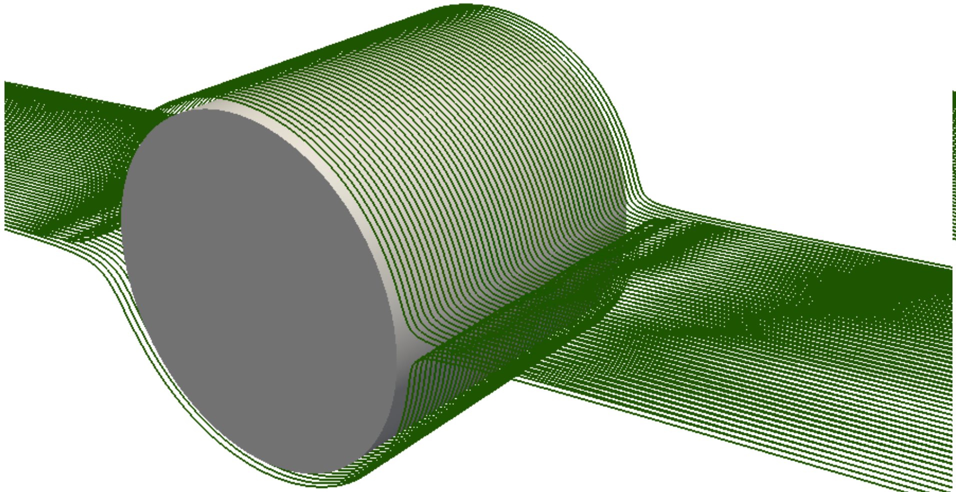

We=1.8

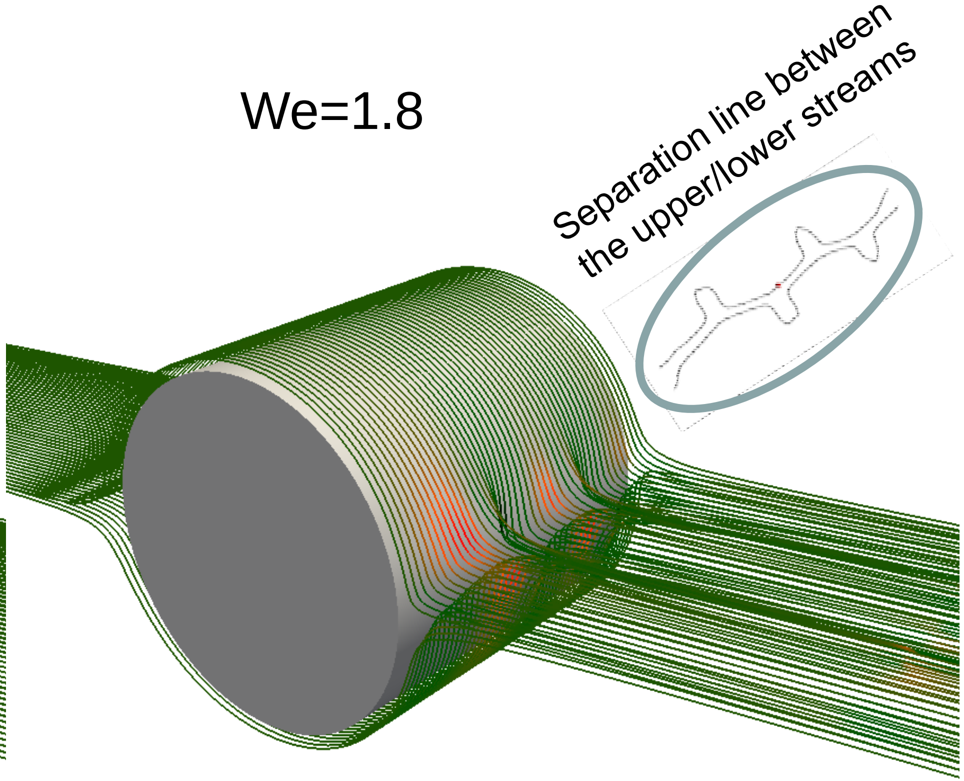

Single phase validation on 2D benchmark "flow around a cylinder"

Reference: Damanik et al.

	Shear thining n=0,75				Shear thickening n=1,50			
	Damanik*		Our results		Damanik*		Our results	
level	C_D	C_L	C_D	C_L	C_D	C_L	C_D	C_L
1	3,20082	-0,01261	3,20450	-0,01215	13,6209	0,34250	13,6233	0,34347
2	3,26433	-0,01342	3,26637	-0,01347	13,7380	0,35052	13,7379	0,35037
3	3,27739	-0,01342	3,27755	-0,01343	13,7688	0,34941	13,7688	0,34928

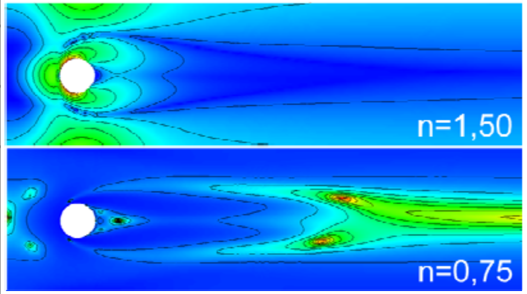

Viscosity distribution

Pseudo 2D rising bubble in Power-Law fluids

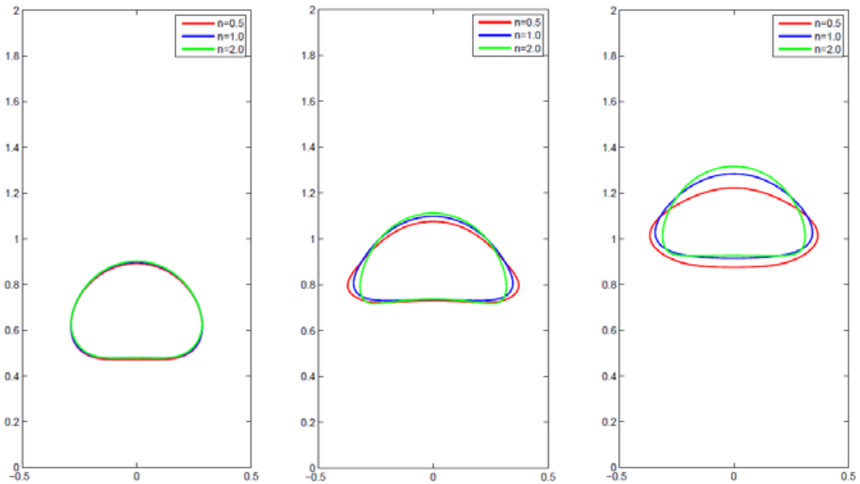

Mesh converged bubble shapes for n = 0.5, 1.0, 2.0

Droplet generation for Power-Law fluids

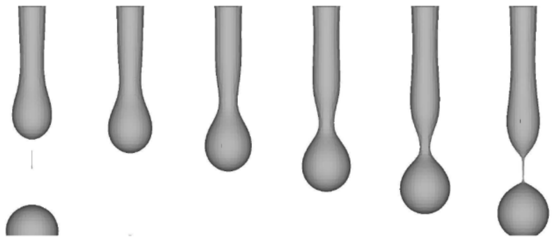

Jet formation n=1.0

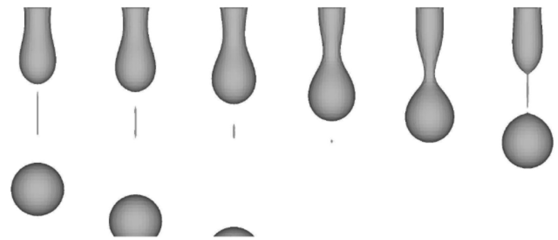

Dripping n=0.5

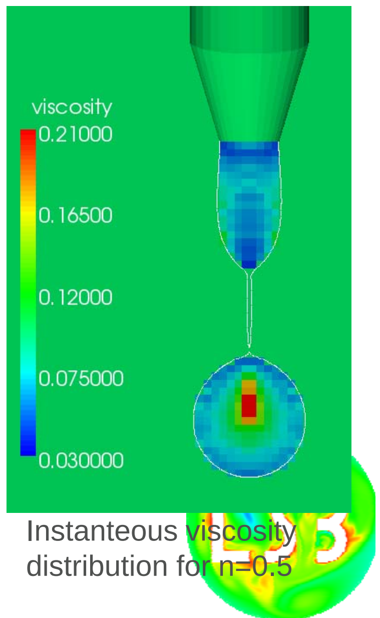

Instanteous viscosity distribution for n=0.5

Viscoelastic Multiphase Flow

Preliminary numerical results – 2D rising bubble

Material 1: Viscoelastic fluid described by the Oldroyd-B model

Material 2: Newtonian fluid

Test case	ρ_1	ρ_2	μ_1	μ_2	$\mathbf{g}$	σ
1. Viscoelastic ($\Lambda = 10$)	10	0.1	10	1	9.8	0.245
2. Newtonian ($\Lambda = 0$)	10	0.1	10	1	9.8	0.245
3. Viscoelastic ($\Lambda = 10$)	10	0.1	2	1	9.8	0.245
4. Newtonian ($\Lambda = 0$)	10	0.1	2	1	9.8	0.245

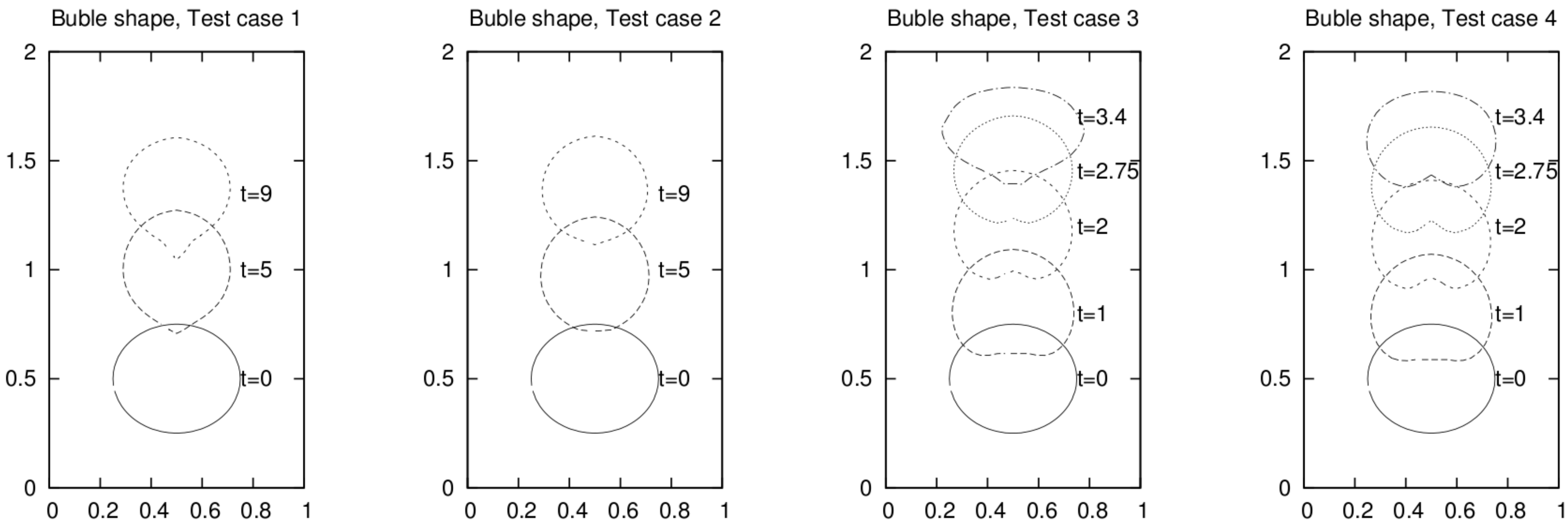

Encapsulation Processes

- Numerical simulation of *micro-fluidic drug encapsulation ("monodisperse compound droplets")*
- Polymeric "bio-degradable" outer fluid with generalized Newtonian behaviour
- Optimization w.r.t. boundary conditions, flow rates, droplet size, geometry

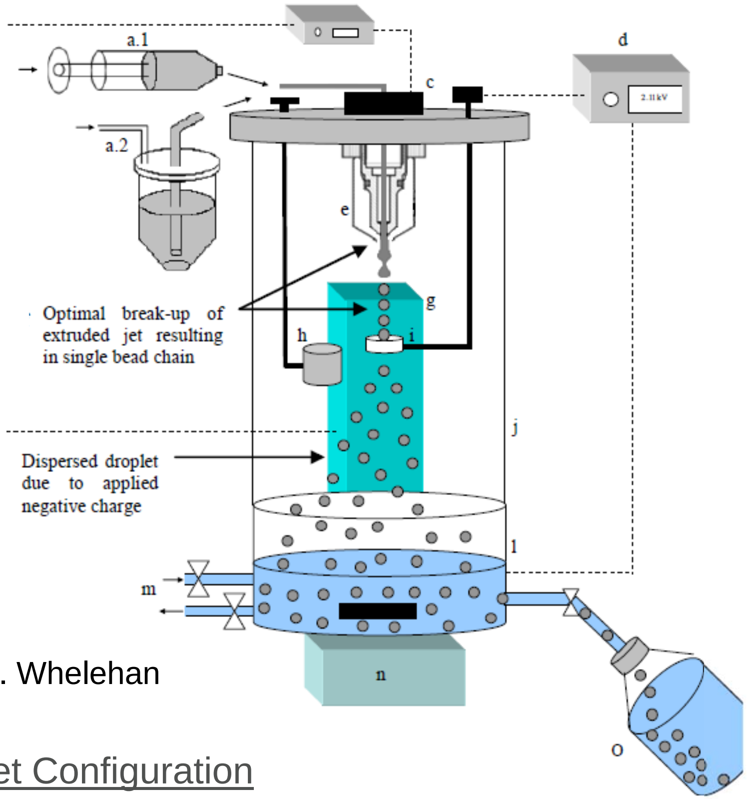

M. Whelehan

In Pharmaceutics

- Controlled drug release
- Protection of chemically active ingredients (from both sides)
- Protection against shear stress in stirred reactors
- Protection against evaporation
- Taste or odor masking

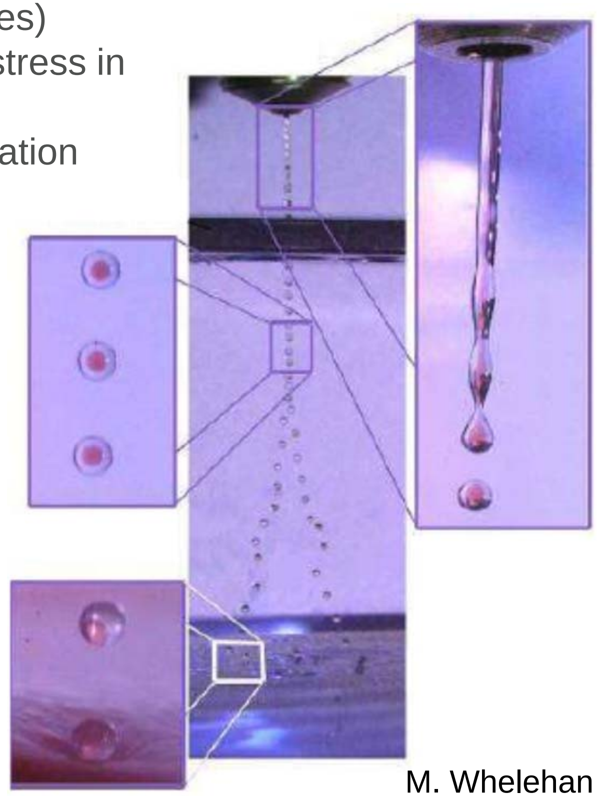

M. Whelehan

Jet Configuration

- Core material is defined as the specific material that requires to be coated (liquid, emulsion, colloid or solid)
- Shell material is present to protect and stabilize the core (Alginate, Chitosan, Gelatin, Pectin, Waxes, Starch)

Encapsulation Processes

technische universität dortmund

	Tasks related to code development	Tasks related to application
mgLS(2)-FBM-FEM flow module	• Multiple Level Set fields for simulation of liquid core encapsulation - l/l/g • Fictitious boundary method for particle encapsulation - s/l/g	• Validation via experimental results • Modulation for monodisperse compound drops

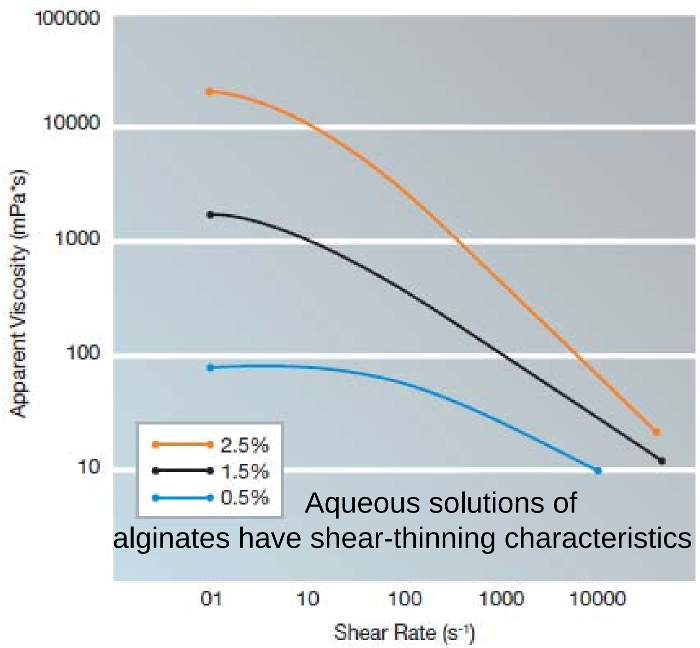

Aqueous solutions of alginates have shear-thinning characteristics

Preliminary simulation results for encapsulation of solid particles

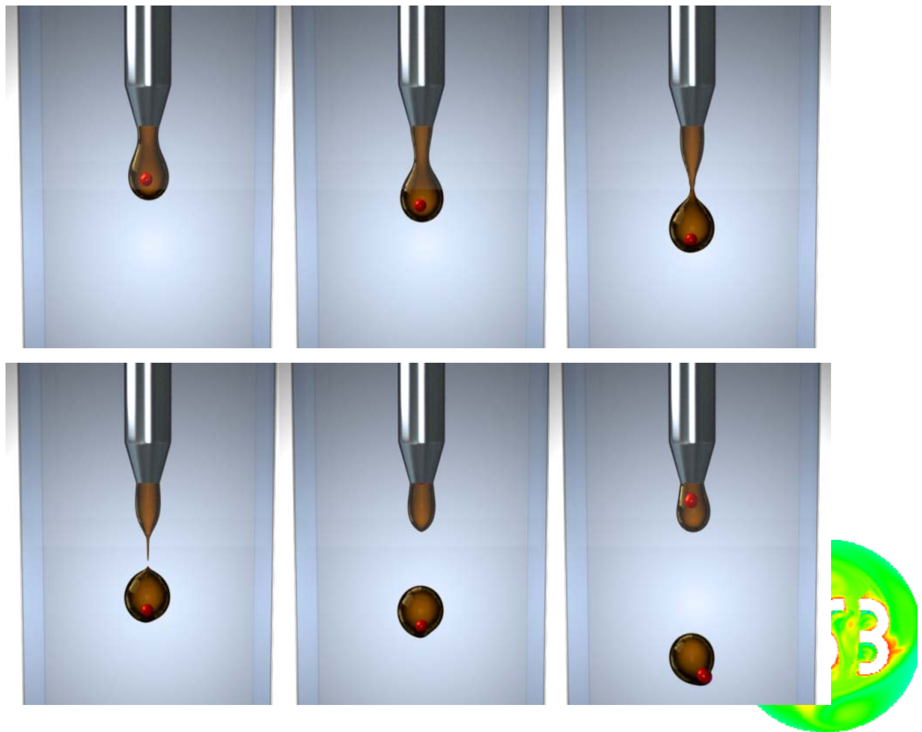

Summary

technische universität
dortmund

Robust numerical and algorithmic tools are available using

- ✓ Classical and Log Conformation Reformulation (LCR)
- ✓ Monolithic Finite Element Approach
- ✓ Edge Oriented stabilization (EO-FEM) and local GDM
- ✓ Fast Newton-Multigrid Solver with local MPSC smoother

for the simulation of nonlinear flow with (extreme) rheological behaviour

Advantages

- ✓ No CFL-condition restriction due to the fully implicit coupling
- ✓ Positivity preserving
- ✓ Higher order and local adaptivity

- **The non-symmetric bilinear forms due to LCR**

$\tau \in T_{PD} \subset \left[L^2(\Omega)\right]^4$ **such that** τ **is positive definite**

$$c(\tau, v) = \int_\Omega \exp(\tau) : D(v)\, d\Omega$$
$$\geq \beta_2 \left\|\exp(\tau)\right\|_{0,\Omega} \left\|v\right\|_{1,\Omega}$$
$$\geq \beta_2 \left\|\tau\right\|_{0,\Omega} \left\|v\right\|_{1,\Omega} \quad \forall \tau \in T_{PD}, \quad \forall v \in \left[H_0^1(\Omega)\right]^2$$

$$\tilde{c}(\tau, u) = -2\int_\Omega B(\nabla u, \sigma_c) : \tau\, d\Omega$$
$$\geq \beta_2 \left\|\tau\right\|_{0,\Omega} \left\|v\right\|_{1,\Omega} \quad \forall \tau \in \left[L^2(\Omega)\right]^4, \quad \forall v \in \left[H_0^1(\Omega)\right]^2$$

Higher Order Nonconforming FEM

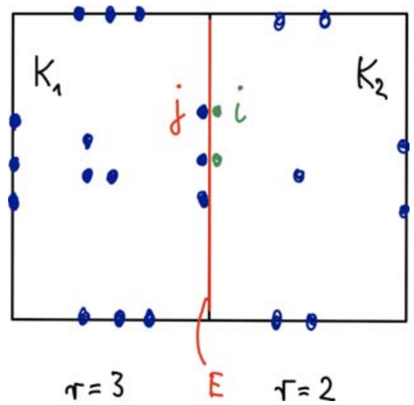

- Larger FE space which allows high order approximation
- d.o.f.s belong to at most two elements which is good for parallelisation
- Coupling of different polynomial orders
  - Mortar condition: test space ≈ order at slave side

$$|E|^{-1}\int_E v_h|_{K_2} L_{E,k}\,ds = |E|^{-1}\int_E v_h|_{K_1} L_{E,k}\,ds, \quad 0 \le k < 2$$

  - No hanging nodes

What are „Extreme Fluids"???